

final report

Project code: B.CCH.6210
Prepared by: Chris McSweeney
Commonwealth Scientific and Industrial
Research Organisation Agriculture Flagship
Date published: August 2015
ISBN: 9781741919547

PUBLISHED BY
Meat & Livestock Australia Limited
Locked Bag 991
NORTH SYDNEY NSW 2059

Measuring methane in the rumen under different production systems as a predictor of methane emissions

Meat & Livestock Australia acknowledges the matching funds provided by the Australian Government to support the research and development detailed in this publication.

This publication is published by Meat & Livestock Australia Limited ABN 39 081 678 364 (MLA). Care is taken to ensure the accuracy of the information contained in this publication. However MLA cannot accept responsibility for the accuracy or completeness of the information or opinions contained in the publication. You should make your own enquiries before making decisions concerning your interests. Reproduction in whole or in part of this publication is prohibited without prior written consent of MLA.

Acknowledgements

The authors wish to thank the Department of Agriculture, Meat and Livestock Australia and CSIRO for project funds. We would further like to acknowledge Professor Kourosch Kalantar-Zadeh and his team at the Royal Melbourne Institute of Technology for their collaboration on the project as well as Dr Gonzalo Martinez for his assistance with cattle respiration trials at Lansdown Research Station, and Steve Austin and Jagadish Padmanabha for their technical support.

Executive summary

The livestock industries require a technology to rapidly and accurately measure enteric greenhouse gas emissions from individual animals under grazing conditions. Intra-rumen devices incorporating gas sensors and a wireless sensor network platform have been developed that log concentration of methane, carbon dioxide and hydrogen gas in the rumen for research purposes. The devices are equipped with a novel gas permeable membrane embedded with silver nanoparticles which allows the diffusion of the target gases while blocking corrosive hydrogen sulphide. Real time data from the capsule in the rumen can be relayed via an ear tag to a remote personal computer using the public G3 network communication system. Power supply to the device enables data logging for approximately a month when the sampling rate is set at 20-30 minute intervals. The diurnal fluctuations in fermentation-gas production associated with feeding events were accurately monitored. Concentration of hydrogen in the rumen appears to reflect production rate but this relationship could not be established for methane. Measurement of a marker gas released at a constant rate in the rumen will be needed to estimate methane production for assessment of methane abatement methodologies and genetic selection programs.

Table of Contents

Acknowledgements	2
Executive summary	3
1. Background	5
2. Methodology	6
3. Results and discussion	31
4. Conclusions	60
5. References	61
6. Future research needs	61
7. Publications	62

1. Background

Gas production in the rumen of livestock provides an important indication of metabolic function, as well as being a significant contributor to the anthropogenic greenhouse gas problem. The livestock industries require technology to measure enteric methane emissions from large numbers of individual animals simply, quickly, accurately and reliably to enable researchers and producers to develop, monitor and validate methane mitigation strategies to reduce emissions from grazing ruminants. Current technologies, such as respiration chambers and the sulphur hexafluoride (SF₆) tracer method, have limitations which make it difficult to reliably measure genetic and field variability and the effects of diverse farm management practices. As a result, there are currently no methods available to accurately and reliably measure methane production from large numbers of grazing animals. Techniques for enteric methane emission measurements on individual animals can be classified into direct and indirect measurements. Direct measurement methods include total or partial enclosure of animals, whereas indirect methods include the use of tracers (isotopic and non-isotopic) and estimations based on rumen fermentation characteristics (Pinares-Patino *et al.*, 2007; Pinares-Patino and Clark, 2008). The use of respiration or methane chambers (direct measurement) and the sulphur-hexafluoride (SF₆) tracer (indirect measurement) technique (Johnson *et al.* 1994a, 1994b) to measure methane emissions from ruminant livestock *in vivo*, are the two most widely used methods. In theory, the SF₆ technique is ideal for grazing ruminants, but often when large numbers of animals are involved ($n > 50$), large variability between and within animals on consecutive days have been recorded, especially when sheep have had little or no prior training with the apparatus. On the other hand, respiration chambers have greater sensitivity than tracer techniques, but they are not easily transportable, are usually limited to one animal at a time, and can be very expensive to construct.

After reviewing the appropriate technologies to justify research for methane measurements on grazing livestock, the recent availability of miniaturised infrared sensors, coupled with the technological advances made with wireless platforms, have now made this idea possible. Thus, it was concluded that the best option was to use commercially available sensors (infra-red, electrochemical, semi-conductive) for methane, carbon dioxide, and hydrogen. These sensors could be integrated with the CSIRO-Pervasive Autonomous Communications Platform (PACP) with telemetric capability and the sensors powered with their own 3.7 V battery supply. The complete unit would be small enough for insertion into a gas diffusible capsule which would reside inside the rumen. Once inside the intra-rumen diffusion cells, the sensors would be protected from the corrosive environment of the rumen, but would still be able to collect and transmit measurement data from the equilibrated gases to the outside of the animal. This project developed and refined these new gas diffusion cells and electronic sensor technologies and tested their ability to provide a robust method for measuring gas concentrations (i.e. methane, hydrogen and carbon dioxide) from individual ruminants with sufficient accuracy, low labour demand and simple data acquisition to allow large scale screening of animals for methane emissions to discriminate phenotypic differences and effects of variation in feed base, climate and management. This work

involved collaboration between researchers at CSIRO Agriculture Flagship, CSIRO Digital Productivity and Services Flagship and the Royal Melbourne Institute of Technology (RMIT).

2. Methodology

Design of infra-red (IR) gas-sensor devices

1. Housing of gas sensor and electronics

Figure 1 shows the initial housing and end-cap design for the IR gas-sensing device. The main housing was a commercially available polypropylene controlled-release device (CRD) capsule with an end-cap which allowed gas from the rumen to permeate through a gas diffusible polydimethylsiloxane (PDMS) membrane to a sensor on the other side (Figure 2). The end cap included an O-ring seal, a gas diffusible membrane and supporting wire mesh for the membrane. The end-cap slid inside the CRD capsule.



Figure 1. Initial CRD capsule and end-cap design

After extensive testing of the IR gas-sensor device assembly, a number of design faults were identified including;

- Tearing and holes in the PDMS membrane
- Leakage and sealing around the membrane

- Ballooning of the PDMS membrane
- End-Caps are not reusable
- Excessive time involved in gluing the gas sensor round printed circuit board (PCB) to the end-cap
- large gas volume for the end-cap to accommodate the pressure sensor

To solve these issues a new gas sensor device end-cap was designed.

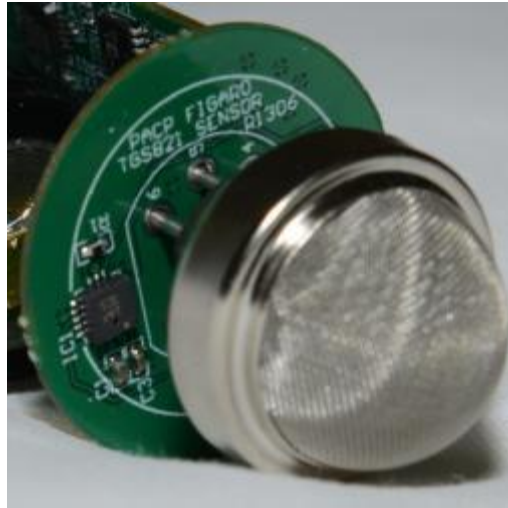


Figure 2. H₂ gas sensor and round printed circuit board (PCB) for measuring pressure

In the initial IR H₂ gas-sensing device, a round printed circuit board (Figure 2), was glued to the inside of the end-cap and separated the gas sensor side of the device from the internal rectangular PCB and battery which was sealed and protected from the rumen gases. The main issue with this design was the quality of the seal of the round PCB to the end-cap was poor allowing rumen gases to leak inside the device and resulted in ballooning and potential rupture of the PDMS membrane.

Figure 3 shows the final assembly diagram for the current IR gas sensor device. The sensor device (sensor, rectangular PCB and battery) and the PDMS membrane are all assembled as a complete unit first before installing into the CRD. The assembled sensor device is pushed into the CRD capsule with a pressure release seal open. When the internal pressure is equalised to the atmospheric pressure the seal is closed. The pressure release seal minimises the ballooning of the PDMS membrane before installing the device in the rumen.

A red cap and optional stainless steel mesh is clipped over the front of the CRD capsule (Figure 4). The stainless steel mesh has a number of advantages including prevention of tearing and holes in the PDMS membrane and the filtering of the pressure port on the end-cap.

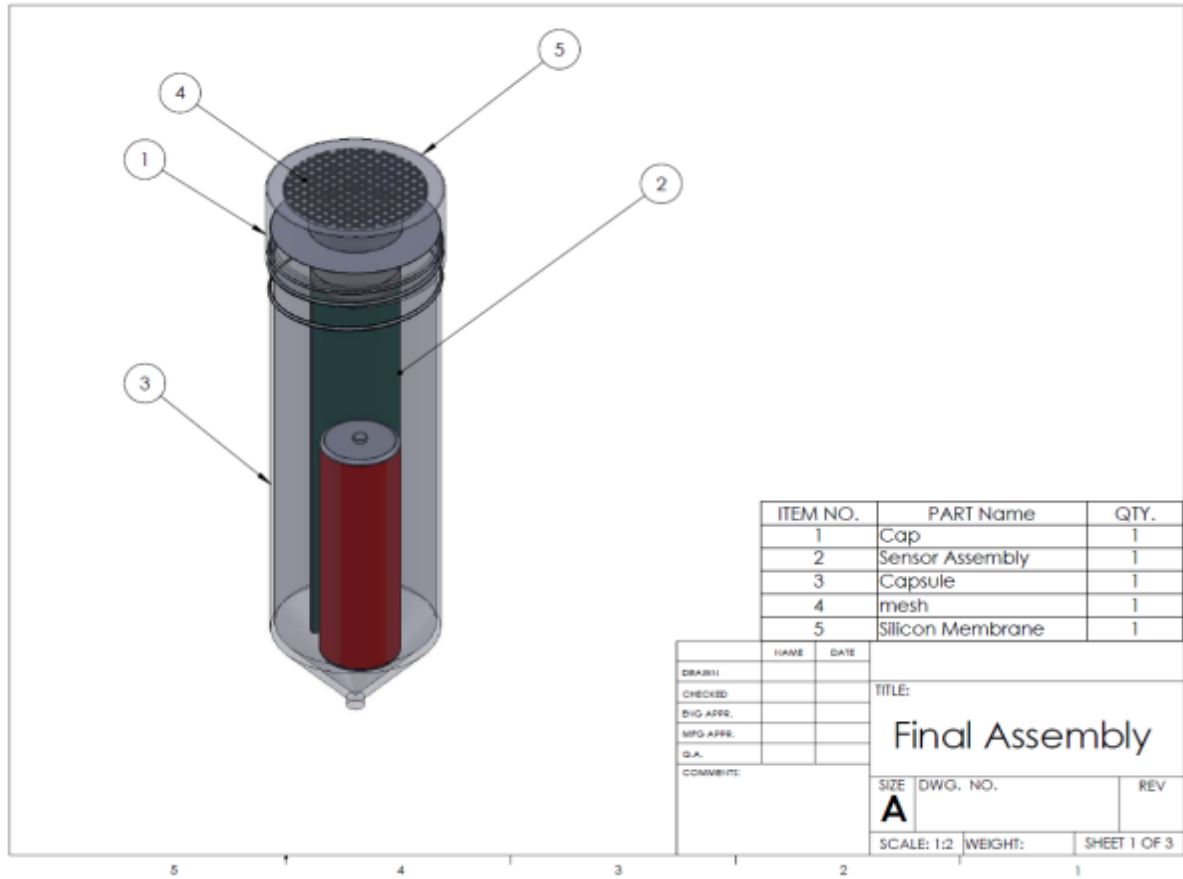


Figure 3. Final assembly design of the current IR gas-sensing device with end-cap, PDMS membrane with supporting metal mesh is mounted onto the front of the gas sensor.



Figure 4. Final assembly of the current IR gas-sensing device with end-cap, PDMS membrane with supporting metal mesh is mounted onto the front of the gas sensor. Pressure port inlet is indicated.

There are a number of parts, as shown in figure 5, that make up the H₂ IR gas-sensor device including;

- New end-cap design
- Rectangular silicone seals for the PDMS membrane
- Compression sleeve and silicon O-ring seal for the domed hydrogen gas sensor
- Two nitrile O-rings to enable the end-cap to seal on the inside of the CRD capsule
- Back plate and two M3 screws to hold the electronic assembly and gas sensor to the end-cap
- Silicone tubing to fit to the pressure port on the end-cap and the pressure release valve
- Red cap and optional stainless steel mesh is clipped over the front of the CRD capsule

The H₂ IR gas sensor device is assembled with silicon lubricant on the O-rings. The whole assembly can be easily assembled and disassembled and reused when required. This also has major advantages in pre and post gas sensor calibration.

The previous device design needed a larger gas volume for the end-cap to accommodate the pressure sensor. The new design has reduced the gas volume and has resulted in faster hydrogen gas response times from the device. The heater in the H₂ gas sensor produces an increased pressure in the CRD capsule. To prevent this increased pressure, a release valve is connected to silicone tubing and pressure port on the end-cap.

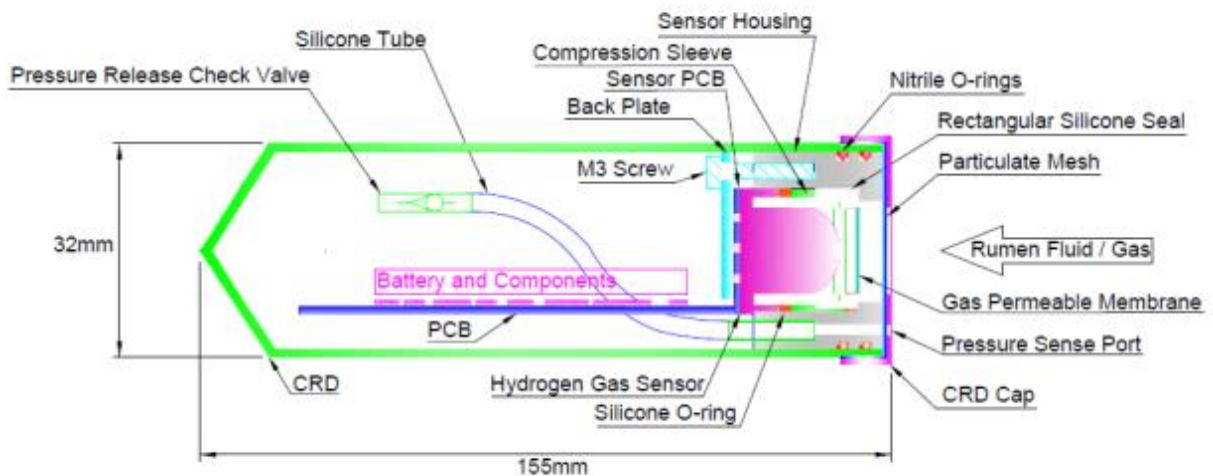


Figure 5. Detail parts of the current H₂ IR gas-sensor device assembly

There are a number of parts, as shown in figure 6, that make up the current CH₄ and CO₂IR gas sensor device including;

- New end-cap design
- Rectangular silicone seals for the PDMS membrane
- Two nitrile O-rings to enable the end-cap to seal on the inside of the CRD capsule
- Back plate and two M3 screws to hold the electronic assembly and gas sensor to the end-cap
- Silicone tubing to fit to the pressure port on the end-cap and the pressure sensor on the PCB
- Red cap and optional stainless steel mesh is clipped over the front of the CRD capsule

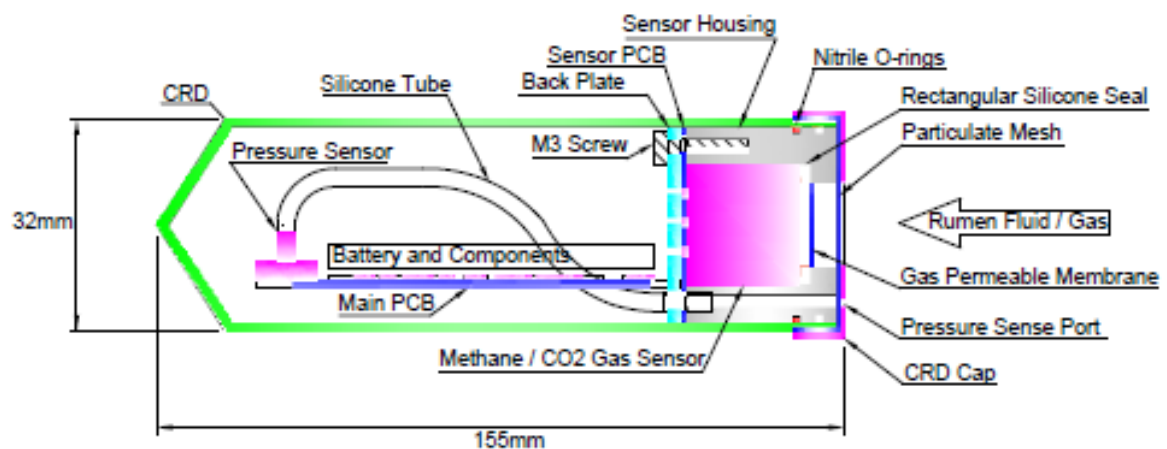


Figure 6. Detail parts of the new CH₄ and CO₂ IR gas sensor device assembly

The CH₄ and CO₂ gas-sensor device is assembled with silicon lubricant on O-rings. The whole assembly can be easily assembled and disassembled and reused when required. This also has major advantages in pre and post gas sensor calibration.

The previous device design needed a larger gas volume for the end-cap to accommodate the pressure sensor. The pressure sensor has now moved to the main PCB with pressure applied with a silicon tube and pressure port on the end-cap. The lower gas volume has resulted in faster gas response times from the device.

There is a small hole in the clip on red cap to expose the pressure port to the rumen (Figure 4). If the stainless steel mesh is used in the red cap it has advantages for filtering the rumen liquid entering the opening of the pressure port. The capillary action of the silicone tube and pressure port prevents rumen liquid from travelling down to the pressure sensor.

Figure 7 shows the gas sensor device assembly which is almost identical to the H₂ IR gas sensor device assembly. The gas sensor is a cylindrical shape instead of a dome for the hydrogen sensor. The compression sleeve and silicon O-ring seal is therefore not required for the CH₄ and CO₂ IR gas-sensor device assembly.



Figure 7. CH₄ and CO₂IR gas-sensor device assembly

The rectangular silicone seal for the PDMS membrane is shown in figure 8. When the end-cap unit is assembled the pink seal has a pressure fit on the inside of the end-cap and the front surface of the gas sensor.



Figure 8. CH₄ and CO₂ IR gas-sensor device showing end-cap seals

2. Gas permeable membranes and anti-corrosive materials

The blocking of H₂S gas molecules entering the capsule and causing corrosion of the sensors was an important technological challenge to making a robust device. Royal Melbourne Institute of Technology (RMIT) under Project B. CCH 6220 (Membrane Development and Analysis) developed a nanocomposite catalytic membrane made of polydimethylsiloxane (PDMS) with different weight concentrations of silver (Ag) nanoparticles catalyst to reactively remove H₂S from CH₄ and CO₂ gas streams. PDMS was chosen as a model base polymer as Ag nanoparticles could be well dispersed into its matrix. At a small Ag nanoparticles loading of 1%, the catalytic membranes were able to remove more than 60% of H₂S gas molecules. Characterization revealed that the exposure to H₂S gas molecules transformed the Ag nanoparticles into a catalytic nano compound made of Ag and Ag₂S. The nano compound then catalytically decomposed H₂S, while it had a much smaller effect on CO₂ and almost no effect on CH₄ gas species (see Final report - BCCH 6220). The presented nanocomposite system demonstrates the ability to efficiently remove H₂S from mixed gas streams (Figure 9).

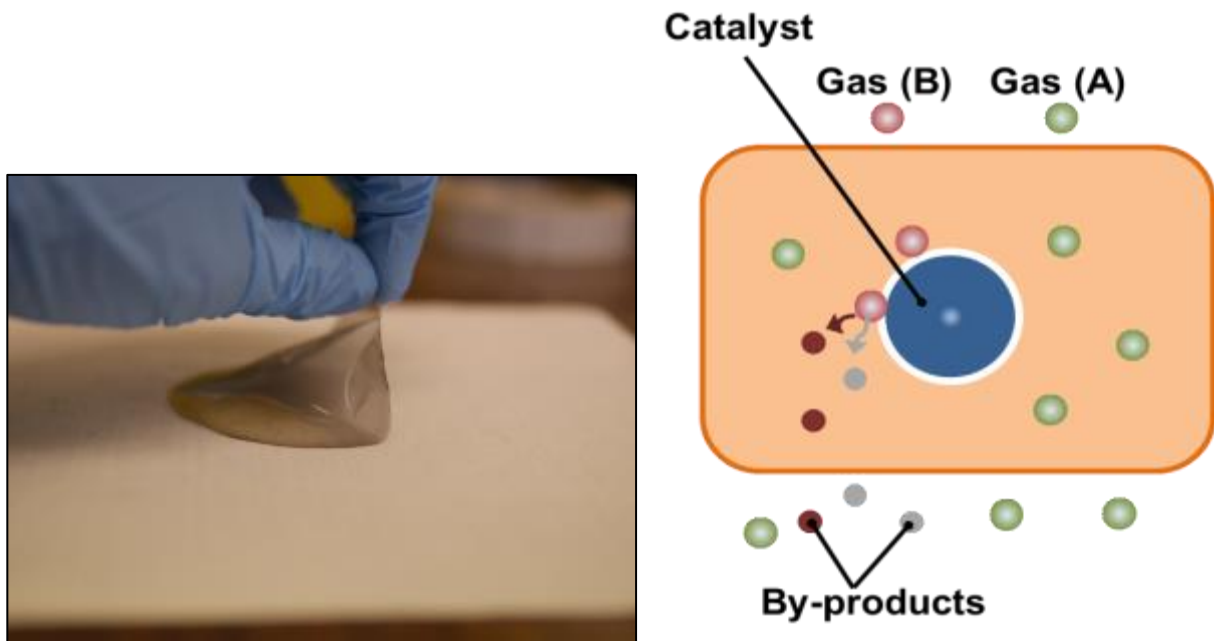


Figure 9. Photograph and schematic diagram of PDMS membrane with embedded Ag nanoparticles for removal of H₂S (Gas B)

Animal Testing A total of 100 PDMS membranes manufactured and supplied by RMIT were sent to the F D McMaster Laboratory, Armidale for testing in animals to determine the degree of fouling by microbial colonisation. The membranes consisted of 5 differing concentrations of silver nanoparticles (n = 20 replicates) to test if the inclusion of Ag nanoparticles overcame or restricted the microbial colonisation on the membrane after a period of time in the rumen of a fistulated steer, ranging from 4 to 28 days. Five membranes, one of each of the Ag nanoparticle concentrations (control, 0.125%, 0.25%, 0.5% or 1% Ag), were secured into 20 nylon bags (Figure 10) and submerged in the rumen for 4, 7, 14, 21 and 28 days. On removal from the rumen the bags were rinsed in phosphate buffered saline (PBS) solution and stored in either PBS or glutaraldehyde solution. Upon completion of the sampling period, all the samples were dispatched to RMIT for either electron microscopy or DNA analysis.

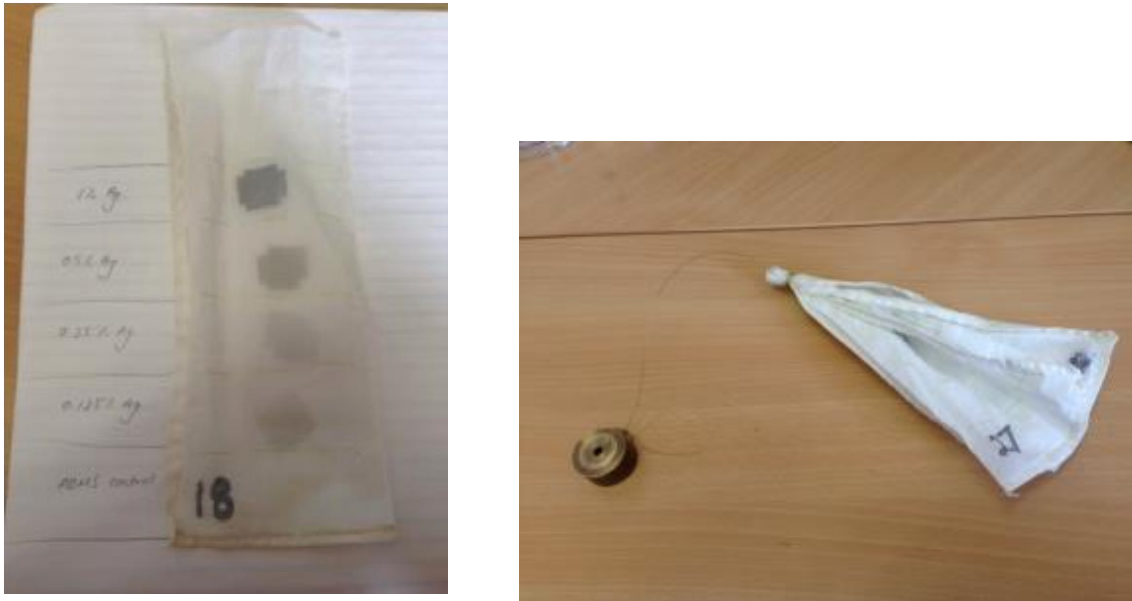


Figure 10. Placement of PDMS membranes in nylon bags for placement in the rumen

3. CH₄ and CO₂ sensor and printed circuit board
 - a. Cattle and sheep intra-rumen sensor

The new wireless CH₄ and CO₂ IR gas-sensor device, shown in figure 12, is based on the PACP (Pervasive Autonomous Communication Platform) circuit board and was designed and developed by the CSIRO Autonomous Systems engineering team. The PACP Salus environmental wireless sensor shown in figure 11 was developed by the CSIRO ICT Centre and was used to conduct an experiment on the humidity, pressure and temperature within a CRD residing in the rumen. Gas measurements may need to be corrected for changes in temperature, pressure and humidity.



Figure 11. PACP Salus environmental sensing device

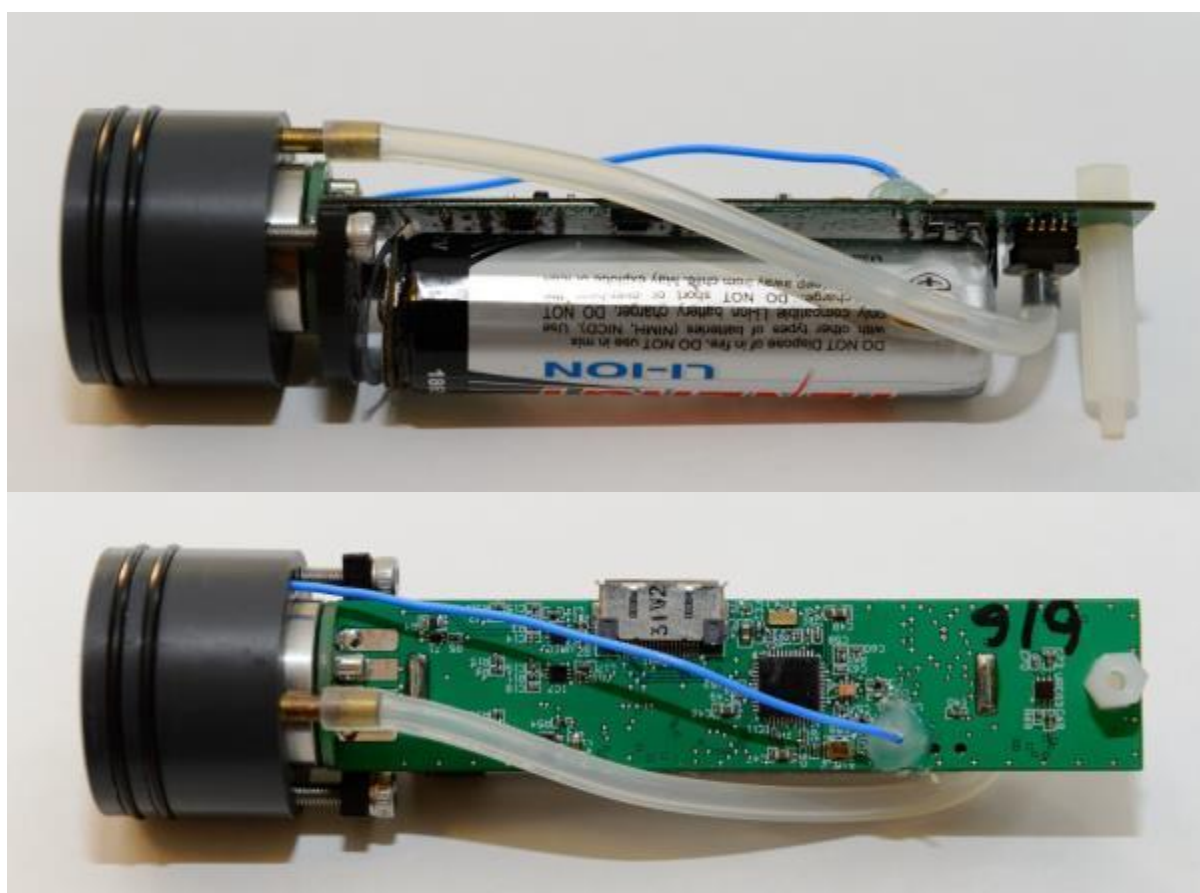


Figure 12. PACP Serqet wireless CH₄ and CO₂IR gas-sensor device

The current IR gas-sensing device PCB has a number of key features and specifications including;

- Socket for one miniaturized infra-red SGX® dual gas sensor to measure 0 to 100% concentrations of methane and carbon dioxide gases.
- Texas Instruments CC430F5137 microcontroller and 916 MHz radio transceiver
- 16-Bit, 8-Channel Serial Output Sampling Analog-To-Digital Converter with precision voltage reference
- Pressure and temperature sensors
- Very low powered gas sensor filter circuits for the reference, methane and carbon dioxide signals
- Gas sensor thermistor for gas sensor temperature monitoring
- Battery voltage, charging voltage and current monitoring
- 32 Mbit serial-interface data Flash memory
- Switchable regulators for the gas sensor and gas circuit power
- Efficient 5 volt step-up converter to increase gas sensor lamp voltage and gas sensitivity readings
- Efficient on-board Li-ion battery charger which can be used for energy harvesting
- 916 MHz quarter wave wire antenna
- Improved radio range from inside the rumen and up to 3 Km line of sight
- Size without end-cap, including the dual gas sensor and battery, is 115 mm long x 20 mm round
- Board mounted rechargeable 3.7 volt @ 2.6 A hour Li-ion battery

The PCB is designed using very small components including 0201 sized surfaced mount capacitors and resistors. A conformal coating is applied to protect the electronics against moisture, chemicals, and temperature extremes inside the harsh environment of the rumen. The miniaturized infra-red SGX® CH₄ and CO₂ gas-sensor is mounted on the gas exposed side of the end-cap. The sensor is protected from the rumen by the RMIT Ag-PDMS membrane. There are eight pin push connectors on the round printed circuit board enabling the easy replacement of the dual gas sensors.

Figure 13 shows a simplified block diagram of the PACP Serqet IR CH₄ and CO₂ IR gas-sensor device. There are six main components to the device including the microcontroller and RF radio transceiver, flash data memory storage, analog to digital converter, gas sensor and amplifiers, sensors and interfaces and the li-ion battery, charger and power supplies.

The CC430F5137 microcontroller and radio transceiver shown in figure 13 provide an interface to the pressure, temperature and dual gas sensors and the on-board flash data memory storage. The radio on the device communicates with receivers external to the animal. The microcontroller can also switch power supplies 'on and off' to the sensor circuits to save power.

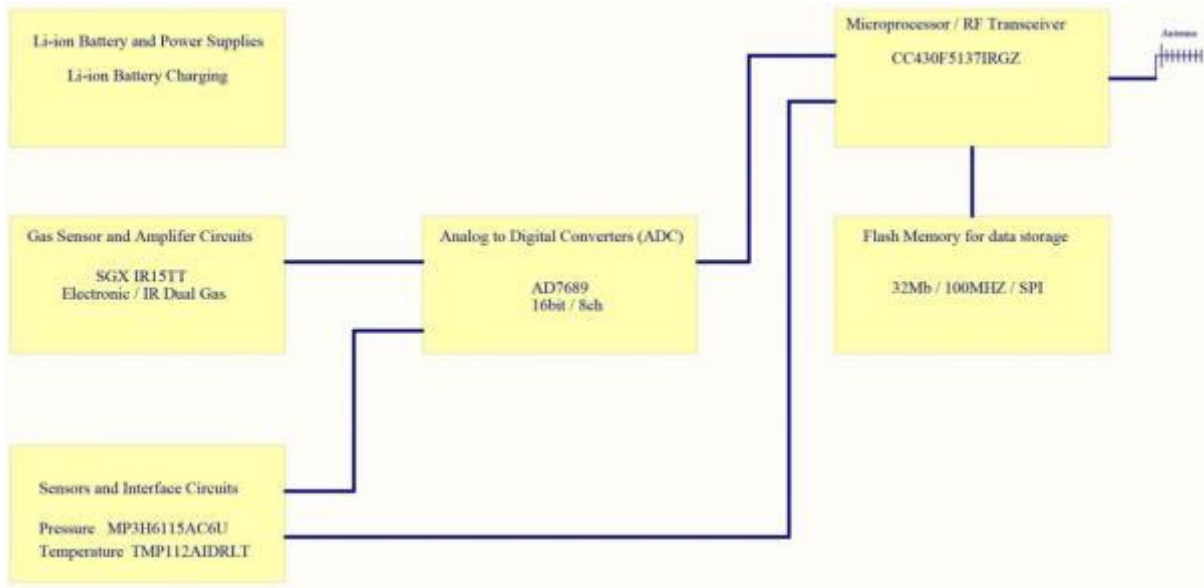


Figure 13. Block diagram of the PACP Serqet IR CH₄ and CO₂ gas-sensor device

When a measurement of CH₄ and CO₂ concentration is required, the microcontroller turns on the power supply to the gas amplifier and heater circuits. A very accurate 5 volt peak to peak 4 Hz square wave is generated for the heater circuit resulting in three 4 Hz sinewave signals feedback from the gas sensor photodiodes. These represent the sensor reference and the CH₄ and CO₂ gas readings. After these signals are amplified and filtered they are sampled by the Analog to Digital Converter (ADC) for the peak to peak voltage of each signal. Digital Signal Processing (DSP) is applied to the calibrated data in post processing to give the CH₄ and CO₂ concentration data.

A pressure sensor reading is produced in a similar way to the gas readings in that the power supply initially needs to be turned on by the microcontroller. A voltage reading is then taken by the Analog to Digital Converter and calibrated in post processing.

The temperature sensor has a digital interface (I2C) to the microcontroller and a reading can be taken at any time as no power supply switching is required and the device can automatically go into low powered mode.

The microcontroller has the option to write the data to the 32Mbit memory flash and/or send the data over the radio when there is two way radio communications available. The software section will expand more on the firmware needed in the microcontroller.

b. New sheep intra-rumen sensor

The new wireless CH₄ and CO₂ IR gas-sensor device designed for sheep (Figure 14) is based on the PACP (Pervasive Autonomous Communication Platform) circuit board and was designed and developed by the CSIRO Autonomous Systems engineering team.



Figure 14. New PACP Pan wireless CH₄ and CO₂ IR gas-sensor device designed for sheep compared to the original PACP Serqet wireless CH₄ and CO₂IR gas-sensor device

The Pan wireless CH₄ and CO₂ IR gas-sensor device has a number of key features and specifications included that are different to the PACP Serqet wireless CH₄ and CO₂IR gas-sensor device including;

- Encapsulated device that does not need a CRD or end-cap
- Inductive battery charging using the Qi inductive power standard
- Pressure sensing has been removed to reduce space
- Over the air radio micro-controller reprogramming
- PDMS membrane and stainless steel mesh glued to the sensor front
- Size including the dual gas sensor and battery, is 90 mm long x 20 mm round
- Board mounted rechargeable 3.6 volt @ 960mA hour Li-ion battery pack

Figure 15 shows the PACP Pan wireless CH₄ and CO₂ IR gas-sensor device including the two Li-ion batteries on top and the inductive charging coil on the bottom.



Figure 15. PACP Pan wireless CH₄ and CO₂ IR gas-sensor device showing batteries and the inductive charging coil

The PACP Pan wireless CH₄ and CO₂ IR gas-sensor device has been design to be swallowed by a sheep and is a similar size to a sheep CRD. Figure 15 shows the two different PACP wireless CH₄ and CO₂ IR gas-sensor devices and a sheep CRD.

The new PACP Pan device is 90mm x 20mm round compared to the PACP Serqet device which is 160mm x 40mm round when placed within the protective cattle CRD.



Figure 15. PACP wireless CH₄ and CO₂ IR gas-sensor devices and a sheep CRD

4. H₂ sensor and printed circuit board

a. Electrochemical hydrogen sensor

The original wireless hydrogen IR sensor device (Figure 16), is based on the PACP circuit board and was designed and developed by the CSIRO Autonomous Systems engineering team.



Figure 16. Original PACP Hydra wireless hydrogen intra-rumen gas sensor device

The miniaturized electrochemical SGX® gas sensor for hydrogen is mounted on one end of the gas sensing device. The IR H₂ gas-sensing device has a number of key features and specifications including;

- Socket for one miniaturized electrochemical SGX® gas sensor to measure 0 to 1000 parts per million (PPM) concentrations of hydrogen gas.
- Texas Instruments CC430F5137 microcontroller and 916 MHz radio transceiver
- 16-Bit, 8-Channel Serial Output Sampling Analog-To-Digital Converter with precision voltage reference
- Pressure and temperature sensing
- Very low powered gas sensor filter circuits for the reference and hydrogen gas signals
- Battery voltage, charging voltage and current monitoring
- 16 Mbit serial-interface data Flash memory
- Switchable regulators for the gas sensor and gas circuit power
- Efficient on-board Li-ion battery charger which can be used for energy harvesting
- 916 MHz quarter wave wire antenna
- Improved radio range from inside the rumen and up to 3 Km line of sight
- Size, including gas sensors and battery, is 100 mm long x 20 mm round
- Board mounted rechargeable 3.6 volt @ 2.6 A hour Li-ion battery

b. Semiconductor hydrogen sensor

The original IR SGX® hydrogen electrochemical gas sensor device has been replaced with a new Figaro® semiconductor gas sensor device shown in figure 17.



Figure 17. New PACP Hydra wireless hydrogen intra-rumen gas sensor device

This was necessary because the electrochemical gas sensors were unreliable within the rumen and accuracy deteriorated over several days. The new IR H₂ gas-sensing device has a number of key features and specifications including;

- Solder on socket for one miniaturized Figaro® TGS-821 semiconductor H₂ gas sensor to measure 0 to 2000 parts per million (PPM) concentrations of H₂ gas.
- Connector between the round gas sensor and main printed circuit boards
- Texas Instruments CC430F5137 microcontroller and 916 MHz radio transceiver
- 16-Bit, 8-Channel Serial Output Sampling Analog-To-Digital Converter with precision voltage reference
- Pressure and temperature sensing
- Very low powered gas sensor filter circuits for the hydrogen gas sensor signals
- Battery voltage, charging voltage and current monitoring
- 32 Mbit serial-interface data Flash memory
- Switchable regulators for the gas sensor and gas circuit power
- Efficient on-board Li-ion battery charger which can be used for energy harvesting
- 916 MHz quarter wave wire antenna and on-board chip antenna
- Improved radio range from inside the rumen
- Size without end-cap, including the dual gas sensor and battery, is 110 mm long x 20 mm round
- Board mounted rechargeable 3.6 volt @ 2.6 A hour Li-ion battery

The PCB design, components, conformal coating and assembly is similar to that described above for the IR CH₄ and CO₂ gas sensor. The H₂ gas sensor is mounted on the round printed circuit board and can be replaced on the main printed circuit board via the inter-board connectors and solder pads.

Figure 18 shows a simplified block diagram of the PACP Hydra wireless hydrogen intra-rumen gas sensor device. There are six main components similar to the dual (CH₄/CO₂) gas sensing device (Figure 13) except for the pressure and temperature sensors.

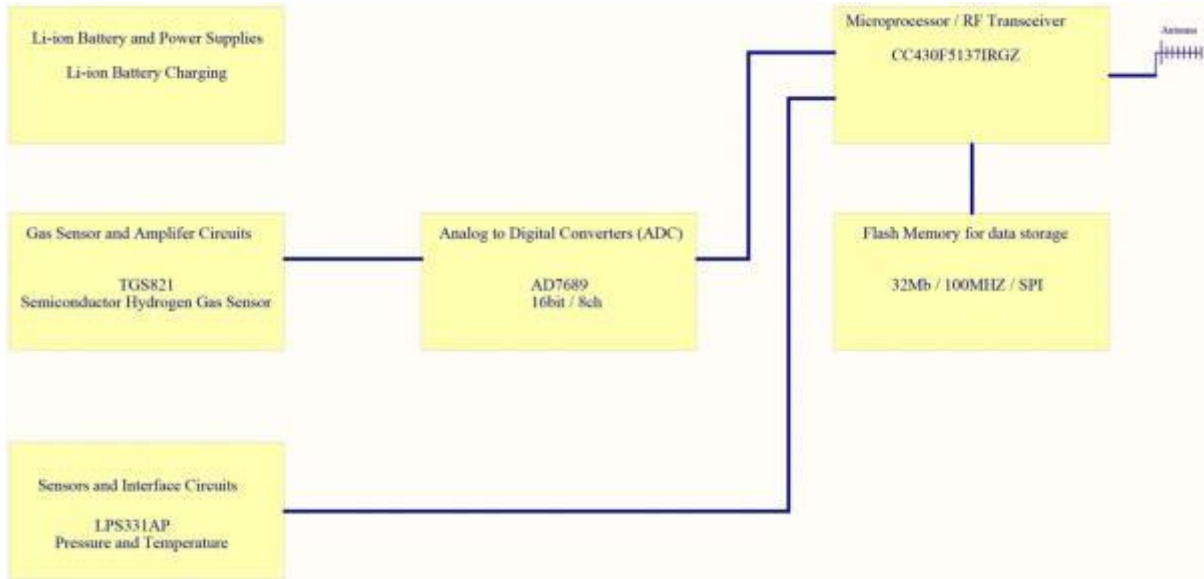


Figure 18. Block diagram of the PACP Hydra IR H₂gas-sensor device

When a measurement of H₂ gas concentration is required, the microcontroller turns on the power supply to the gas amplifier circuits. A very accurate 5 volt rail is supplied to the semiconductor heater circuit resulting in a feedback signal from the gas sensor resistive bridge. The ratio of the gas sensor resistance and a precision reference resistor is amplified and filtered and sampled by the Analog to Digital Converter (ADC). Digital Signal Processing (DSP) is applied to the calibrated data in post processing to give the hydrogen gas concentration data. The pressure and temperature sensor has a digital interface (I2C) to the microcontroller and a reading can be taken at any time as no power supply switching is required and the device can automatically go into low powered mode. The microcontroller has the option to write the data to the 32Mbit memory flash and/or send the data over the radio when there is two way radio communications available.

Software engineering

The sensors used to measure gas concentrations, specifically the CH₄ and CO₂ gas sensor (SGX® IR15TT-R) and the H₂ gas sensor (Figaro® TGS-821), draw approximately 100mW and 660mW, respectively. In typical (non-ruminant) applications, these sensors are connected to mains power so that the devices remain continuously “on”. However, in the intra-ruminal application the sensors must be powered from the finite energy source of a 3.7V (typically 2.6Ahr) Li-ion battery.

Within this fixed energy budget, $P_{battery}$ (typically <10W), continuous operation of the sensors would deplete the batteries in approximately 100 hours (CH₄ and CO₂ IR gas-sensor device) and 15 hours (H₂ IR gas-sensor device) respectively. However, with the aim of being able to measure gas concentrations for up to a month, it is necessary to “duty cycle” the sensor. Only energising the sensor for the minimum period required to get a stable reading before powering the sensor off again. The number of readings that can be obtained is limited. Ideally, the operation of the device should be managed to maximise the

number of readings over the period of interest, and furthermore, the times when the readings are taken should maximise the information/understanding of the rumen gas concentration characteristics. These 2 aspects, as well as the delivery of the sensed information, are the main challenges the software engineering attempts to address.

The minimum settling time will determine what benefit can be obtained and so must be determined for each sensor. The recommended settling time for the CH₄ and CO₂ gas-sensor to achieve operation to “specification” is 30 minutes. However, experimentation revealed reproducible (non-zero) readings were possible after only 48s followed by 5s of sampling. Similarly, the H₂ sensor was found to obtain reproducible results after only 30s of energising.

The average power consumption of the IR gas-sensing device (P_{MCU}), which excludes the gas sensor but includes the processor (microcontroller) and the radio, will become increasingly important as the lifetime of the device is extended. An approximate device lifetime in hours (h) can be modelled via:

$$h = \frac{T_{sample\ period}}{T_{settling}} \times \frac{P_{battery} - P_{MCU}h}{P_{on}}$$

which can be rewritten as:

$$h = \frac{P_{battery}T_{sample\ period}}{(T_{settling}P_{on} + T_{sample\ period}P_{MCU})}$$

where:

h	hours of operation
$T_{sample\ period}$	sample period (time between each measurement)
$T_{settling}$	settling time required for a stable readings for the specific gas sensor
$P_{battery}$	power in Watts available from the battery source
P_{on}	power consumption in Watts while the sensor is “on”
P_{MCU}	continuous power consumption in Watts for the MCU and radio

Note:

$$T_{sample\ period} \geq T_{settling}$$

The denominator term $T_{settling}P_{on}$ is fixed by the sensor employed and apart from determining the minimal settling time, cannot be optimised further. The term, $T_{sample\ period}P_{MCU}$, will depend on the sample period

employed and the continuous energy consumption of the microcontroller unit (MCU) and radio. As $T_{sample\ period}$ becomes larger, the devices operational lifetime becomes increasingly dependent on this second term and so it is important to ensure that P_{MCU} is kept as low as possible. P_{MCU} is dominated by the radio communications strategy employed. Keeping the radio on permits maximum bidirectional communications bandwidth, however continuously consumes approximately 40 mW. This would significantly impact the operational longevity even over short durations (days) and so is not recommended. As such, strategies for reducing the power used for communications are required, and should also attempt to achieve robust delivery of sensed data to an external receiver so that sensed data can be visualised in near real-time via a web interface. The following details strategies to achieve long term robust sensing and communications.

1. Low Power Radio Communication and Data Relay

As previously stated, it is beneficial to reduce that amount of time the radio is on to reduce the power consumption of the IR gas-sensing device. However, when the radio is turned off, there is no mechanism to know whether another device is attempting to communicate with the IR gas-sensing device or not, but this is necessary for multi-hop communications. Therefore, various communications schemes have been developed which attempt to reduce the power required by duty-cycling the radio. Unfortunately, this introduces considerable complexity into the code of the device.

For this research, two approaches have been developed. The first approach achieves close to the lowest power consumption possible for communications, however is single hop. This increases the likelihood that packets will be missed by the receiver (due to the attenuation of the animal) and so a delay-tolerant networking (DTN) algorithm is also required to ensure data was reliably downloaded remotely. As such, the typical operation may not be real-time but delayed until reliable communications directly to the device in the rumen can be achieved.

The second approach known as Wake on Radio (WoR) uses more power on average (though significantly less than having the radio on permanently) but permits multi-hop communications. With a relay device on the animal, but external to the rumen, this approach offers a better chance of delivering real-time data from animals at pasture. To evaluate this approach, a radio compatible ear tag device (developed under another project) was deployed as a relay device (Figure 19) utilising a developed multi-hop protocol that is compatible with the WoR low power radio implementation. Data packets received by the ear tag device are forwarded immediately to a fixed gateway which decodes the compact representation into human readable data and uploads this via a 3G/4G connection into a remote database. This configuration is represented diagrammatically in figure 36.



Figure 19: CSIRO's smart ear tag technology

Figure 20 shows CSIRO's gateway technology which has an embedded computer (Beaglebone Black), 3G modem, 3.6 volt @ 11 Amp hour Li-ion battery pack with solar power or external charging. The unit is connected to a $\frac{1}{2}$ wave 916 MHz radio wave antenna and a high gain 3G antenna.



Figure 20: CSIRO's 3G gateway

For both approaches, the number of packets required to transmit the sensed data to the external receiver can be minimised by ensuring the data is represented in a compact manner. To achieve this a tagged data format (TDF) was employed to pack time-stamped sensor data in a compact representation.

In addition to these software mechanisms for improving the communications robustness, a number of hardware choices are also recommended. Specifically, that the 433MHz or 900 MHz ISM band be utilised and 2.4 GHz bands (such as Bluetooth and Wi-Fi) be avoided due to their high attenuation by animal tissue. Additionally, the directionality of the antenna used should be carefully considered since the orientation of the device in the rumen with respect to an ear-tag or gateway is likely to be random. Two antenna designs are supported by the IR gas-sensing device and were evaluated.

The first approach used a $\frac{1}{4}$ wave whip antenna, however, the semi-directional (toroidal) RF propagation pattern may produce periods where the orientation causes high signal loss. A second approach used a chip antenna with a more omnidirectional (spherical) RF propagation pattern, however, the signal strength in any direction is typically less than that of the whip antenna design.

A series of experiments (1-5) were performed to investigate the connectivity characteristics of the new intra-rumen device design, the CSIRO smart ear tag device as a potential relay device, and CSIRO's gateway technology on fistulated sheep. In these experiments, the ear tag periodically transmits a packet. If the packet is received by the rumen node, it records the received signal strength (dB) to on-board memory. Additionally, the gateway records when a page has been successfully downloaded (which requires 9 round-trip communications per page). Any packets received at the gateway, either directly from the rumen node or via the ear tag, are recorded with the number of hops the packet took before reaching the gateway. For the experiment configurations below, it follows the maximum hop count should be 2 and the minimum be 1.

Relay Experiment 1: CSIRO's smart ear tag on the steer's ear, IR gas-sensing device with the on-board chip antenna and CSIRO gateway

Relay Experiment 2: CSIRO's smart ear tag on steer's fistula, IR gas-sensing with the on-board chip antenna and CSIRO gateway

Relay Experiment 3: CSIRO's smart ear tag on sheep's fistula, IR gas-sensing with the on-board chip antenna and CSIRO gateway

Relay Experiment 4: CSIRO's smart ear tag on sheep's fistula, IR gas-sensing with the $\frac{1}{4}$ wave whip antenna and CSIRO gateway

Relay Experiment 5: CSIRO's smart ear tag on sheep's ear, IR gas-sensing with the $\frac{1}{4}$ wave whip antenna and CSIRO gateway

Additional analysis of the robustness of the hardware and software functionality through experiments focussed on rumen measurements rather than the operation of the device. Some of these experiments were conducted under relatively controlled conditions, while others occurred in the rumen of animals.

2. Adaptive Sampling: Energy Management Supervisor Module

The gas sensors consume up to 3000 times more energy than the pressure and temperature sensors used in the device. Initially a fixed periodic sampling schedule was used for all sensors and it was observed that changes in the low power sensors were correlated with changes in the gas concentrations. This led to the innovation of decoupling the sample rates of the gas and other sensors allowing each individual sensor a periodic sampling schedule that can be dynamically set via the radio. This allowed low power sensors, such as temperature and pressure, to be sampled at much higher frequencies with negligible impact on the lifetime of the device and furthermore, these frequently sampled sensors can be used to schedule when the high power gas sensors are sampled.

The effectiveness of this approach was validated with a dynamic sampling strategy contrasted with a fixed periodic sampling strategy. Both approaches utilised the same number of samples within the same finite period, however the distribution of the samples differed. The information loss was characterised by the squared error from an actual gas concentration trace sampled at a relatively high sample rate. This demonstrated that changes in pressure could be used to trigger when to power the gas sensor to achieve an optimal representation of the gas concentrations over the period. A disadvantage of this approach was that there were typically less samples of high transition events after sustained periods of stable readings.

3. Improving longevity through utilisation of improved battery technology

Recent advances in battery technology are providing batteries with greater energy capacity within the same size battery (i.e. increased energy density) and this trend is likely to continue, if not accelerate, in coming years. At the start of this research, the best-in-class Li-ion battery that would fit into the CRD was the Tenenergy® 18650 3.7 V @ 2,600 mAh Li-ion battery. This battery was used for all in-rumen experiments except for one experiment specifically designed to verify that improvements in battery technology could be readily utilised if needed. A Redilast® 18,650 3.7 V @ 3,400 mAh battery was tested against a Tenenergy® 18650 3.7 V @ 2,600 mAh using CH₄ and CO₂ gas-sensing devices deployed into a fistulated steer at pasture. The sample rates for gas, temperature and pressure sensors were set to 3-minute interval on both devices before they were inserted into the animal's rumen via the cannula. After 10 days the devices were removed and data downloaded. The Redilast® battery provided an additional 30% more energy than the Tenenergy® and is recommended for the IR gas-sensing devices.

Animal Experimentation

Studies were performed in sheep (Armidale) and cattle (Townsville) to measure the performance of the IR gas-sensing device when placed in the rumen. Some studies involved measuring the changes in concentration of gases (CH₄, CO₂ and H₂) throughout a day in relation to feeding while others compared these observations with measurements of gases expired by the animal in a respiration chamber.

1. Sheep studies

Sheep (Merino × SAMM wethers; 57-74 kg live weight) fitted with BarDiamond rumen cannulae were fed once daily (~8:00am) with a pelleted Lucerne (*Medicago sativa*) ration (Ridley pellets®, 18-20% crude protein, 8.9 MJ/kg DM) in individual feed troughs with rations based on maintenance requirements (20 g/kg live weight/d) and adjusted accordingly to establish suitable experimental conditions as per the experimental protocol. Feeding of experimental rations commenced several days before measurements to establish a constant equilibrium in the gut at the time of measurement of gas emissions and before placing animals in chamber studies for similar measurements. IR CH₄ and CO₂ gas-sensing devices were assembled following calibration with certified gases and despatched to Armidale for deployment. During the respiration chamber studies, gas sensing devices were introduced into the rumen via a cannula for measurements over several days. A series of trials of the IR H₂ gas-sensing devices incorporating either the electrochemical or semiconductor type gas sensor were also undertaken in fistulated sheep in respiration chambers at Armidale (Chiswick Research Station).

Methane, carbon dioxide and hydrogen emissions from sheep were performed using four independent open-circuit respiration chambers with volumes of ~1,500 L per unit, fitted with large perspex panels in all the walls, roof and rear door to allow 360° visibility for each animal. The integrated gas analyser, flow meters, software and interface to a PC compatible computer (Oxymax ventilation system) were purchased from Columbus Instruments® (Columbus, Ohio, USA). Gas emissions were calculated by measuring gas concentrations taken from a sample line for each chamber and finally performing a background measurement from within the chamber room facility. The background gas measurement is used to subtract background gas levels from the gas emission values for each chamber at the conclusion of each measurement cycle (1 – 4 chambers). The time to complete a full cycle of measurements for 4 chambers and a background measurement is around 9 – 10 minutes. Gas emissions are reported either as concentration (ppm) or production rates (mg/hr) as well as summed to provide a cumulative measurement for the whole 23 hr experimental period. The Oxymax ventilation system comprised a 0-500 LPM Mass Flow Controller 1% FS accuracy (calibrated to STP 760 mm/0° C) and a 0-500 LPM ventilation blower for each respiration chamber. Gas analysers in the Oxymax System comprised a single beam NDIR CO₂ sensor (0-1%), an Oxymax IR methane sensor (0-1,000 ppm) and a H₂ sensor (0-2,000 ppm). The Oxymax Gas Monitoring System was calibrated before each experimental run using a zero standard (N, 1,000 v/v) and the following certified gas standards O₂, CO₂, CH₄ and H₂ (21.7% ± 0.4%, 0.974 ± 0.022%, 966 ± 27 ppm and 920 ± 19 ppm respectively; AirLiquide, Sydney, Australia). Recovery

rates of injected methane into the chambers (1200 mL CH₄) ranged between 87-93% over a series of tests.

2. Correlation between in-rumen gas concentration and gas cap measures in sheep

In-vivo studies were undertaken to understand the anomaly between amounts of methane peaking post feeding in respiration chambers with decreases in concentration of methane relative to carbon dioxide observed with the intra-ruminal device. The intra-ruminal device has consistently demonstrated methane concentrations in the rumen to peak much later in the feeding cycle at a time when carbon dioxide was at nadir levels during a normal 24 hour cycle (Figure 21). Although changes in relative gas concentrations of CH₄ and CO₂ could arise due to the different PDMS membrane permeation rates for CH₄ and CO₂ (90 versus 1300 Barrer), diffusion coefficient (170 versus 110×10^6 cm²/s) and solubility coefficient (40 versus 400×10^2 cm³/cm³ atm) (Tremblay *et al.* 2006), further studies were needed to ascertain if these observations could be supported by independent measures of gas cap concentrations in the rumen.

Experimentation was undertaken on three fistulated sheep to establish ratios CH₄, CO₂ and H₂ in the gas cap of sheep, fed a once daily ration as in previous respiration chamber experiments to cross reference gas measurements taken by the devices *in vivo*. Gas samples were taken in triplicate at 1.5, 3, 5, 7, 9, 12 and 24 hours post feeding and stored in evacuated containers for gas chromatography analysis. The mean of the duplicates was expressed as the ratio of the gases.

3. Cattle studies

Field Experimentation utilizing fistulated cattle Evaluation of intra-ruminal devices in cattle at the Mc Master Laboratory, Armidale has been undertaken over the life to the project. A small group of four mature fistulated Jersey steers ranging in weight between 508-644kg have been set stocked in a 10ha paddock consisting of improved temperate pasture species of phalaris, ryegrass, fescue and white clover. Adjacent to the paddock is a small set of cattle yards comprising a holding yard and a race which is used to accommodate 2 animals at a time for deploying intra-ruminal devices and also retrieving the units at the completion of experimentation. To overcome variation in positioning of devices, individual intra-ruminal CRDs which house the gas measuring devices were weighted with brass rod (100g) in order to stop them from floating on the grass raft and gas cap and to keep the units fully immersed within the rumen digesta.

Intra-rumen dual gas (CH₄, CO₂) and H₂ sensor device testing in high and low methane emitting cattle

An opportunity to measure high and low methane emitting cattle at Lansdown Research Station (Townsville) with the gas sensor devices became possible in conjunction with project (BCCH 7610). Fistulated cattle were undergoing treatment with a methane inhibitor whilst being monitored for GHG emissions in respiration chambers (Servomax system). The methane inhibitor used in the study was chloroform in a cyclodextrin complex.

Four fistulated Brahman steers (*Bos indicus*) were used in the first *in-vivo* experiment. Animals were fed a forage:grain only diet and were adapted to the diet over 17 days. On days 9 and 10 animals were placed into open-circuit respiration chambers for measurement of CH₄ and H₂ production. Following the initial adaptation/control period, animals received a low dose of chloroform-CD (1.6 g/100 kg LW) for 10 d and for the last two days were confined in open-circuit respiration chambers for direct measurement of CH₄ and H₂ production.

Methane and hydrogen emissions were measured using four independent open-circuit respiration chambers with volumes of ~19.000 L. Gas measurements were performed by Servomex 4100 analyser and Servomex Chroma (Servomex Group Ltd, Crowborough, UK) calibrated by BOC (Sydney, NSW, Australia) standards at zero (N, 999: 1000 v/v); and CH₄ and H₂ with 97.3 and 100 ppm, respectively. Database management was handled by Genesis II hardware (Innotech, Brisbane, Qld, Australia) using digital inputs/outputs at 4–20 mA and the Structured Query Language, while daily CH₄ emissions were calculated by averaging 48-h measurements during each sampling period.

IR CH₄ and CO₂ gas-sensing devices sensors were assembled following calibration with certified gases and despatched to Townsville for deployment. During the respiration chamber phase of the experiment gas measurement devices were introduced into the rumen via a cannula for the final 2 days. A series of trials of the IR H₂ gas-sensing devices incorporating a semiconductor type gas sensor were also undertaken in fistulated cattle in respiration chambers at Lansdown Research Station.

3. Results and discussion

Measurements of Methane and Carbon dioxide by the IR CH₄ and CO₂ gas-sensing device in-vivo

Correlation between IR gas-sensing device readings and gas cap measures

Measurements of rumen gas cap samples taken manually demonstrate a similar gas profile to that observed with the IR device (Figure 21) with the ratio of CO₂:CH₄ peaking shortly after feeding and CO₂ levels nearly 2.5 times greater than that of CH₄ (Figure 22). The gas ratio then declines over time to a point when at 23 h post feeding the concentration of CH₄ exceeds that of CO₂. Note the peak in CH₄ concentration prior to feeding and at a point where CO₂ concentrations are close to reaching the lowest concentration during the diurnal pattern associated with once daily feeding (Figure 23). Interestingly, the ratios of CH₄:H₂ and CO₂:H₂ exhibit a very different profile over the 24h period (Figure 23). They are both relatively low after feeding and increase throughout the day to peak 12- 23h later. The CH₄:H₂ ratio increases in a linear fashion over the period (24 h) between feeding, while the CO₂:H₂ increases linearly for 12 h and then remains at that level until the next feed. This probably indicates that fermentation rate from 12-24h after feeding is slow and H₂ levels are very low but methane continues to be produced at lower levels. There is an increase in rumen temperature of about 1°C which coincides with feeding and a rapid increase in fermentation.

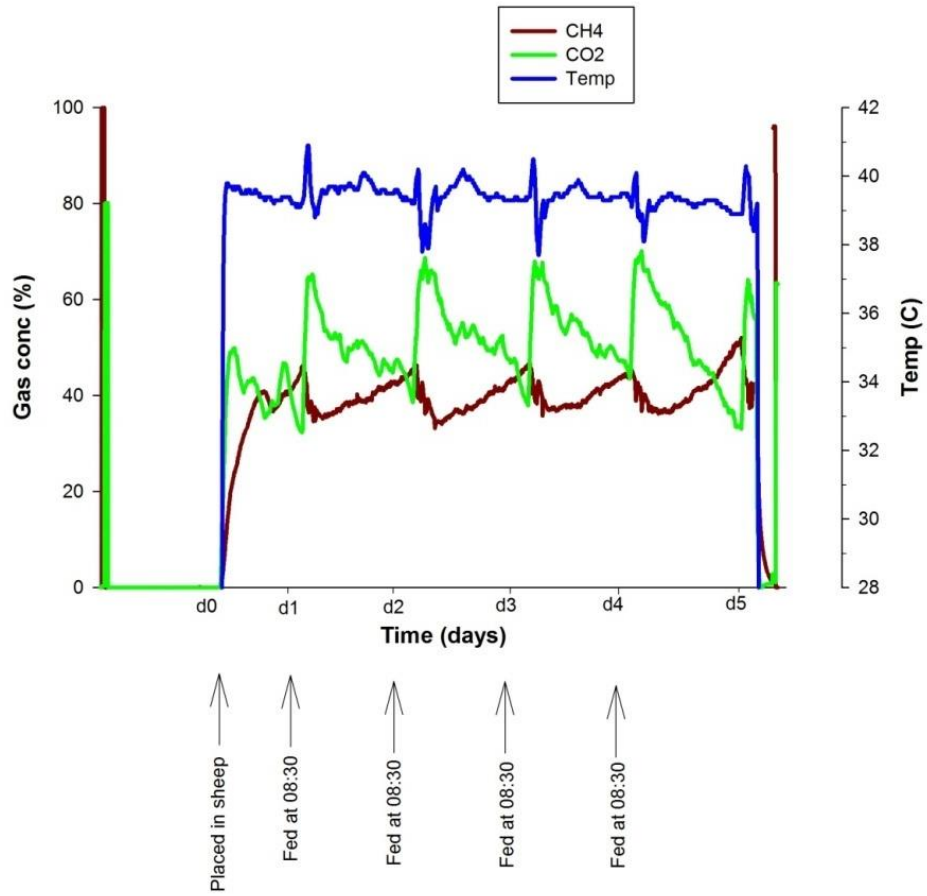


Figure 21. Gas concentration and temperature in the rumen of a sheep as measured by the IR CH₄ and CO₂ gas-sensing device

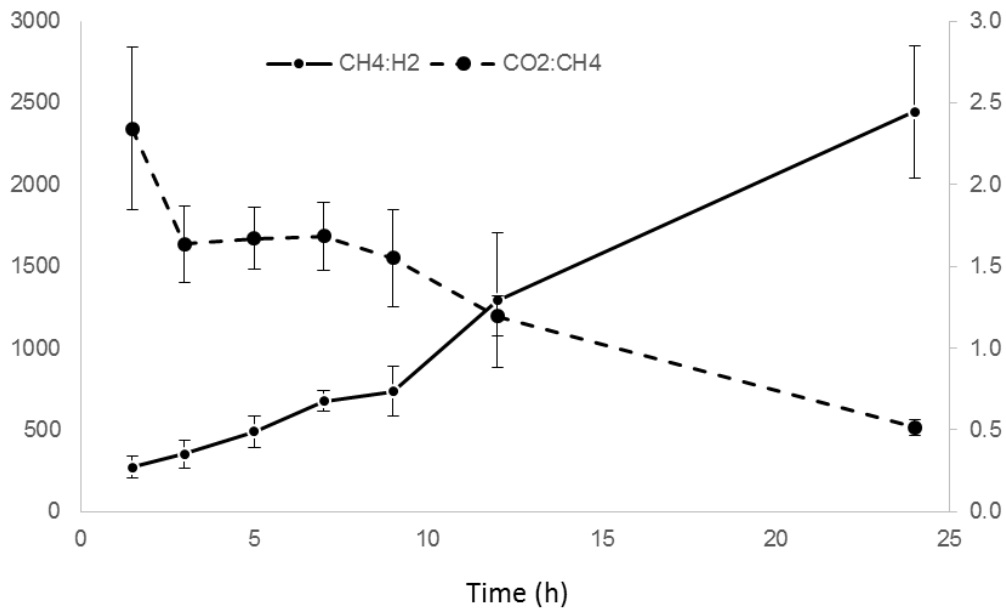


Figure 22. Ratios of rumen gas cap concentrations (CH₄:H₂, solid line; CO₂:CH₄, dashed line) in sheep in response to a single feeding event at the commencement of the 24 hour study. Data represents the mean of 3 animals with vertical bars demonstrating standard errors associated with each time point. Ratio units for H₂ are expressed on the left hand axis.

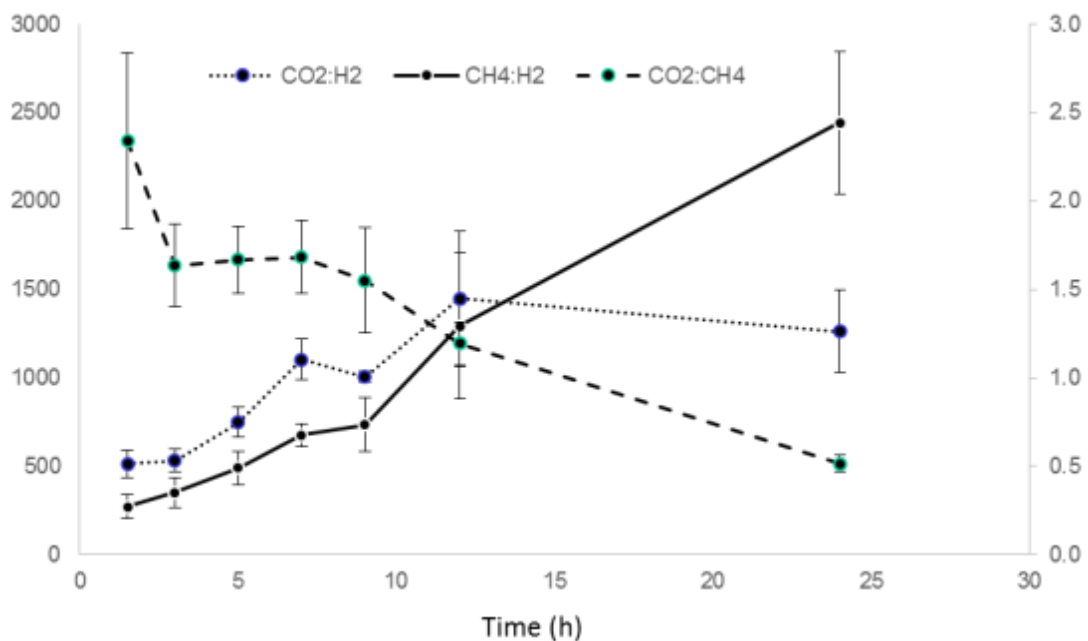


Figure 23. Ratios of rumen gas cap concentrations (CO₂, H₂, CH₄) in sheep in response to a single feeding event at the commencement of the 24 hour study. Data represents the mean of 3 animals with vertical bars demonstrating standard errors associated with each time point. Ratio units for H₂ are expressed on the left hand axis.

Due to differences in diet (roughage hay) the cattle demonstrate a less dynamic gas profile than that of sheep fed lucerne pellets due to delayed and slower fermentation (Figures 24). However, the ratio of CO₂:CH₄ for the cattle is consistent with that observed in sheep with methane concentrations relative to carbon dioxide peaking late in the day.

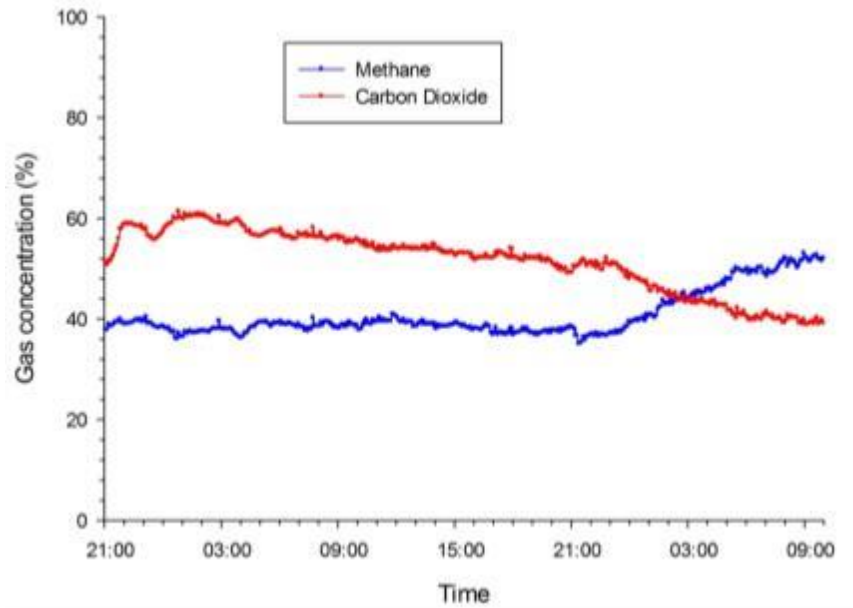


Figure 24. Methane (blue line) and carbon dioxide (red line) concentrations measured by the IR gas-sensing device in a steer

After a period of about a week in the rumen of a sheep, the performance of the sensor declined at varying rates for the two target gases. For CH₄ and CO₂, the change in gas concentration as measured by recalibration with certified gas standards was approximately 4% and 20% respectively for two sensors although the data could be corrected for this drift in calibration (Figures 25). While the PDMS membrane has provided protection for the sensor against H₂S other factors (moisture, volatile compounds etc) still appear to be contributing to spoilage of the sensor. Further design modifications such as placing a gas scrubbing agent e.g. activated charcoal and silica gel crystals) between the PDMS membrane and the sensor may alleviate the spoilage.

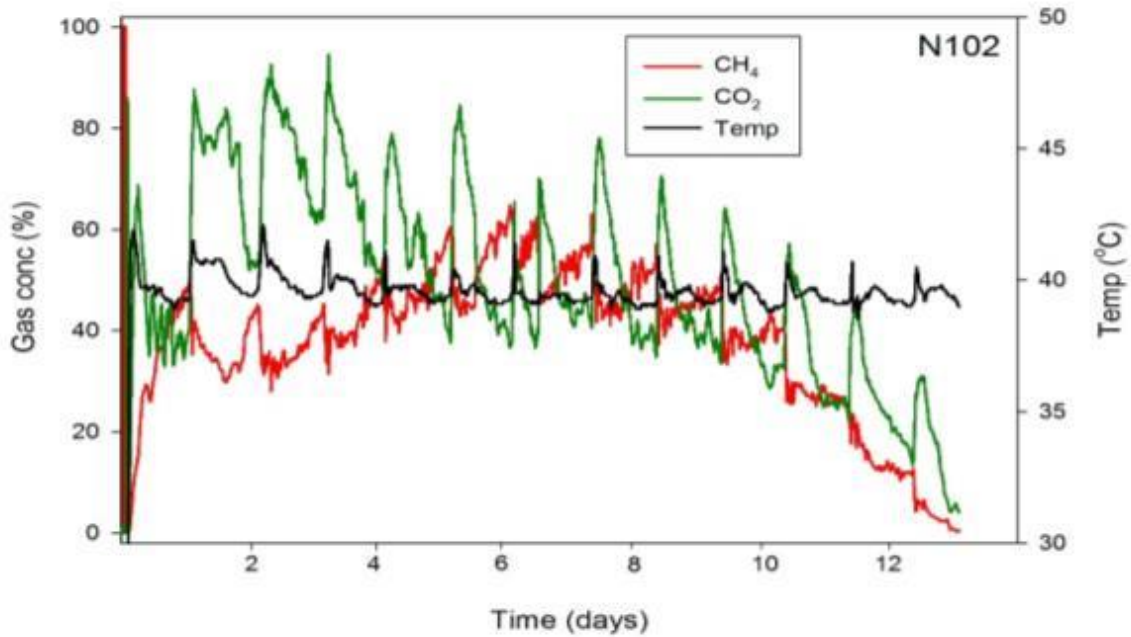


Figure 25. Gas concentration and temperature in the rumen of a sheep as measured by the IR CH₄ and CO₂ gas-sensing device

The repositioning of the pressure sensor on the distal end of the PCB and a modified end-cap to accommodate these changes appear to be working successfully. Pressure values fluctuate between 1050 and 1100 hPa in a steer fed a roughage diet although temperature responses to feeding and fermentation are less pronounced than for sheep fed lucerne pellets (Figure 26). Measurements within the rumen were taken every 20 seconds throughout the 48h period and show considerable variation every 3-4 readings. The improved capability in measuring variation of pressure in the rumen is considered adequate for use in addressing the influence of pressure variation on the infrared gas sensor output values. This variable is now available for use in improving the accuracy of estimating absolute gas concentration in the rumen from the raw sensor output data.

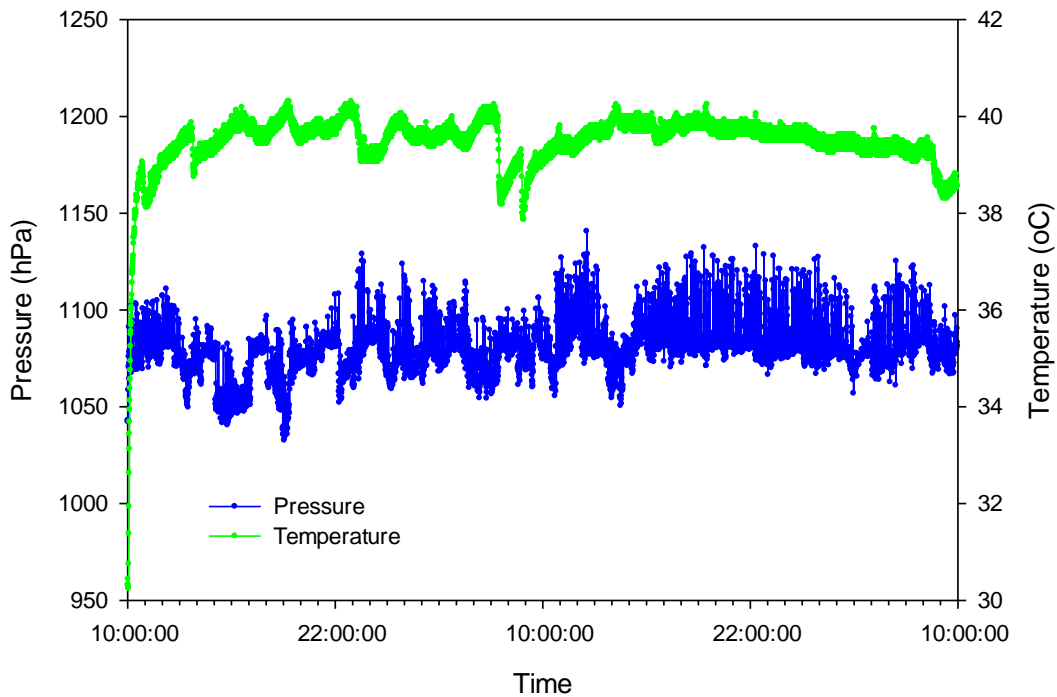


Figure 26. Temperature and pressure measurements taken in a steer fed a roughage diet at 10:00 hours daily.

Measurements of hydrogen by the IR gas-sensing device in-vivo

Electrochemical hydrogen sensor

The electrochemical SGX-e2v® hydrogen IR gas-sensing device was trialled in sheep and cattle for a period of one week. The sheep were fed once per day in the animal house while the cattle grazed pasture. The hydrogen concentration and temperature were measured and compared against the animal feeding events. This allowed for the examination of a relationship between the time of feeding and the various parameters measured.

Hydrogen levels rose sharply soon after the sheep were fed in the morning and then declined (Figure 27 a&b). A temperature peak occurred just prior to the hydrogen peak which was consistent over 6 days of testing. Likewise the hydrogen response was consistent following once daily feeding for the whole experimental period; however the size of the hydrogen response declined after 4 days in all animals (Figure 27a). Under grazing conditions in cattle (Figure 28), the hydrogen peaks were less pronounced and occurred later in the day when the major feeding activity occurred (Gregorini, 2012). The rise in temperature due to gut fermentation generally peaks at around the middle of the night, which may be associated with rumination activity. These findings contrast to earlier observations made on housed sheep fed a once daily ration in the morning.

It was apparent that the accuracy of the device was compromised after about 4 days and appeared consistent. These experiments have demonstrated that due to the harsh environment of the rumen the electro-chemical gas sensors are not suited for long term monitoring but are probably accurate as a research tool for shorter terms studies in fistulated animals. A global search of alternative commercial hydrogen sensors identified the Figaro TGS821 hydrogen semiconductor sensor device as a suitable alternative and therefore the project designed and tested a IR hydrogen Gas-sensing device incorporating the Figaro sensor.

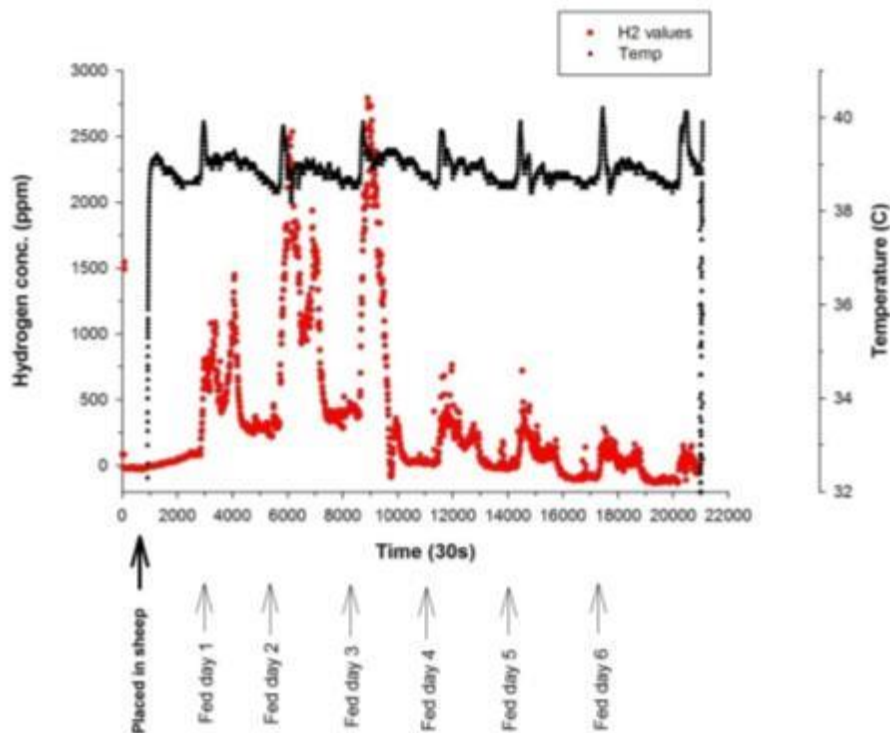


Figure 27a.Hydrogen gas concentration and temperature in the rumen of a sheep for a 7 day period.

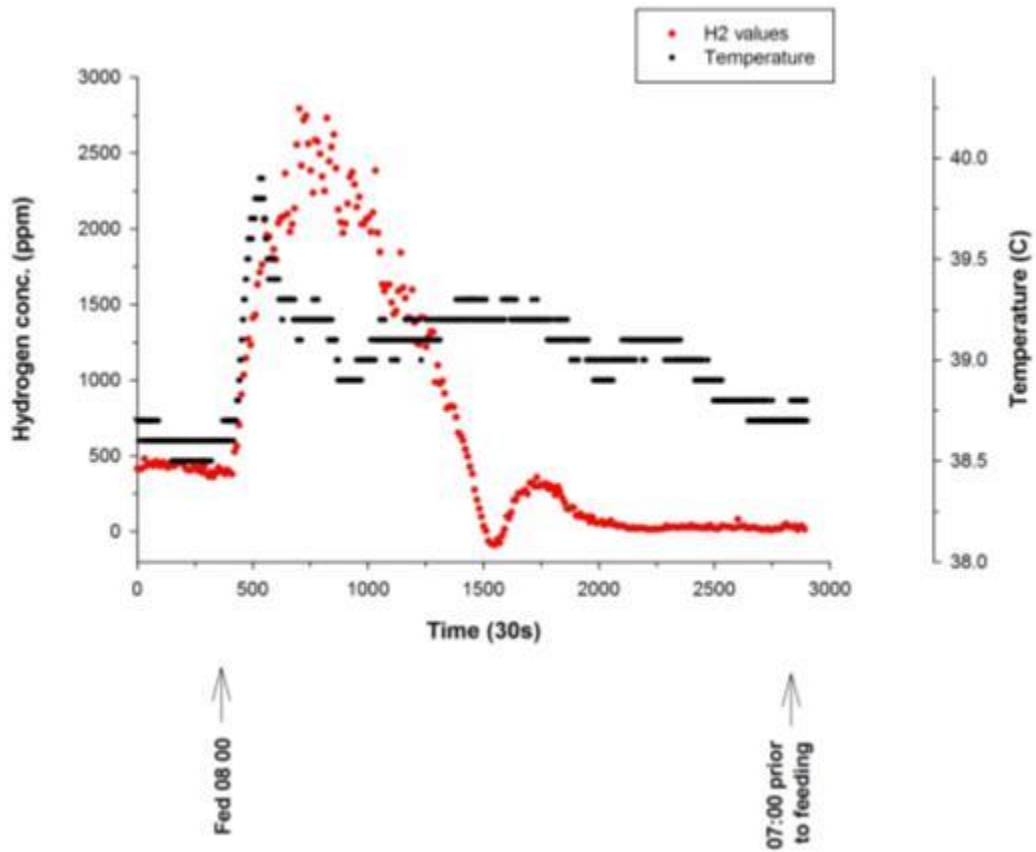


Figure 27b. Profile of diurnal variation in hydrogen concentration and temperature in the sheep rumen in relation to once daily feeding measured by the IR hydrogen gas-sensing device.

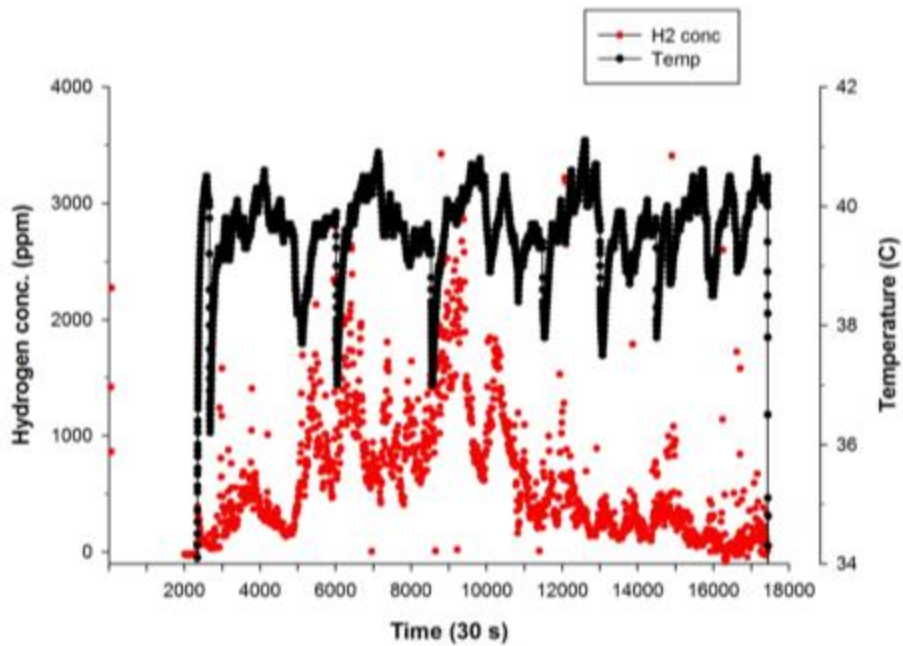


Figure28. Hydrogen gas concentration and temperature in the rumen of steer at pasture.

Figaro TGS821 hydrogen semiconductor sensor device experiments

Respiration chamber data of eructated hydrogen gas from both sheep and cattle demonstrate a significant rise shortly after feeding and then a rapid decline associated with methanogen activity. It would be expected that the rapid decline in hydrogen gas values as measured by the intra-ruminal device should mirror that of the respiration chamber data, however in our recent studies, this was not always the case (Figure 29). Studies with the TGS-821 hydrogen gas sensor in cattle demonstrated a rise in hydrogen levels in the rumen associated with feeding a roughage:grain diet (60:40) (Figure 29), however, unlike the respiration chamber data, hydrogen gas concentration did not always return to baseline values in the latter part of the day (Figure 29). Results from both sheep and cattle in chambers have consistently demonstrated a peak in hydrogen gas levels after once daily feeding, which declines quickly once readily fermentable substrate is depleted. As seen in Figure 29, hydrogen gas levels rise quickly soon after deployment into the rumen via the cannula in response to feeding. Hydrogen levels decrease later in the day to levels at the detectable limit of the respiration chamber gas analyser. As the volume of the cattle respiration chamber is approximately 20,000 litres, the dilution of the gas in the chamber volume is such that the concentration of hydrogen is often below the detectable limit of the respiration chamber gas analyser post-feeding. This has also been observed in the sheep chambers (1,500 litres volume), where there is a more pronounced hydrogen peak and a more rapid decline in concentration. When the same sheep was fed 1000g or 500g Lucerne pellets a rise in hydrogen concentration was usually recorded by the IR hydrogen sensor but this was not always consistent. All sheep had resting levels of about 80-150 ppm H₂ which was below the detection level of the respiration chambers (Figure 30).

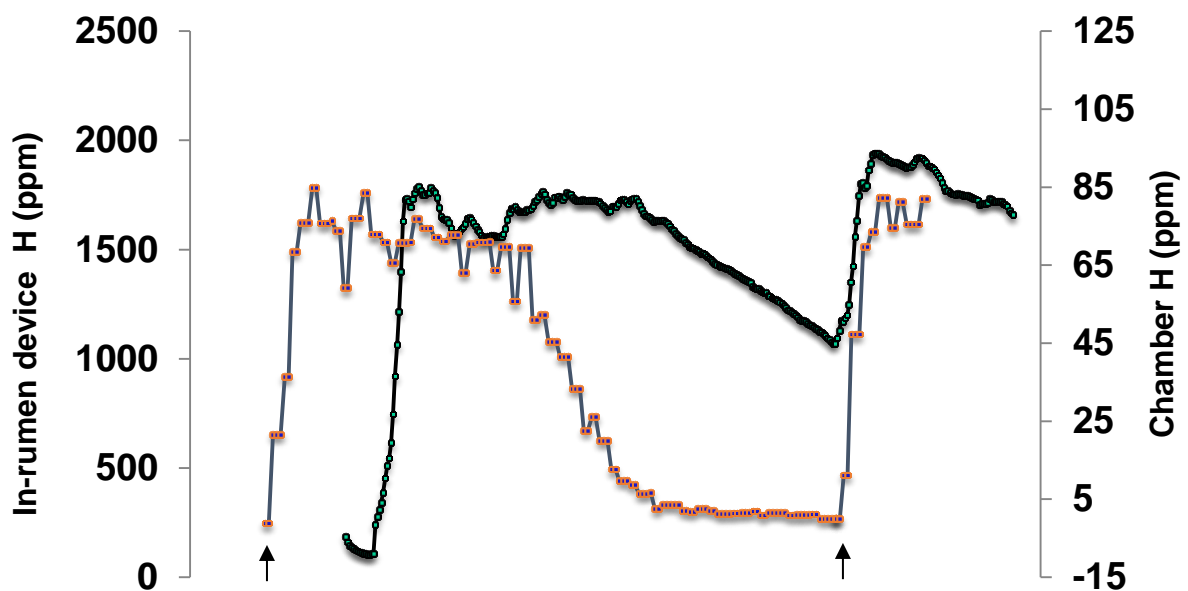


Figure 29. Hydrogen concentration in the rumen of cattle measured with the intra-ruminal device (black line) and measured as eructated gas via the respiration chamber (red line). Arrows indicate feed offered at 24 h interval

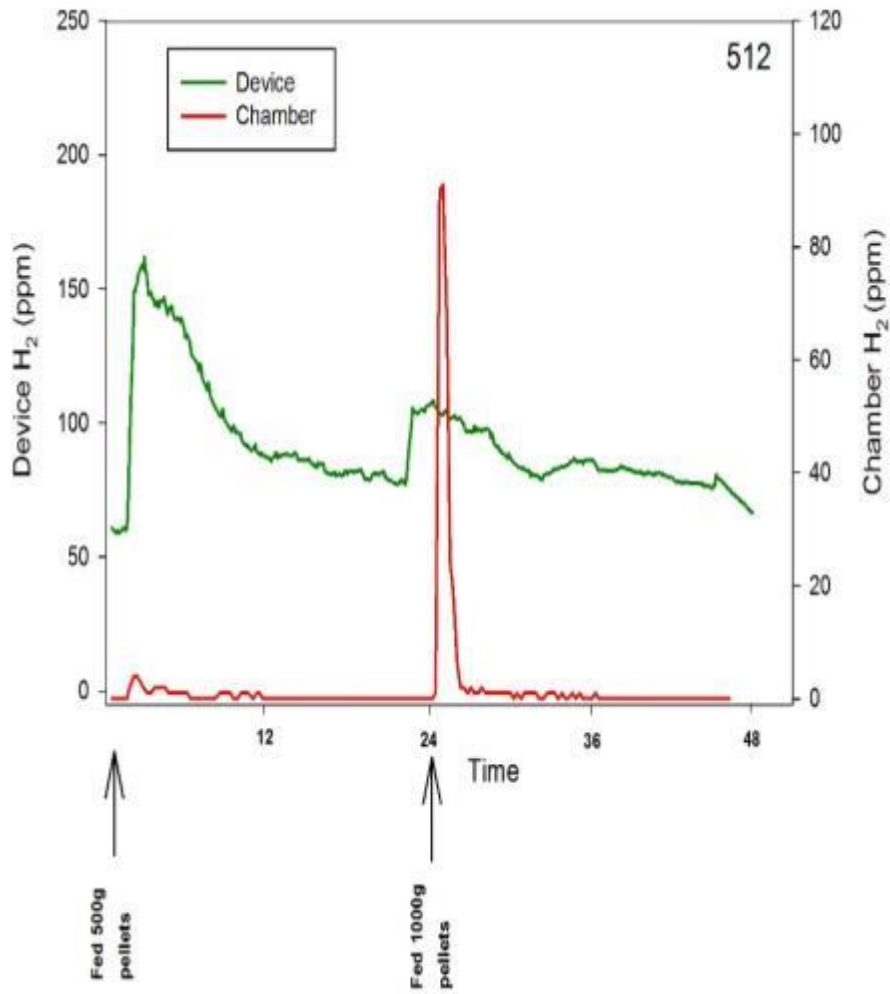


Figure 30. Hydrogen concentration measured with the intra-ruminal device and measured as eructated gas via the respiration chamber in sheep fed 1000g or 500g of Lucerne pellets on alternative days.

To examine this anomaly between the intra rumen sensor and respiration chamber hydrogen measurements, a series of *in-vitro* studies were carried out at RMIT both in the presence and absence of oxygen (Figure 31) to determine why the sensor values did not always return to baseline. Although not specified by the manufacturer, there appears to be a need for oxygen gas to clean the sensor for optimal performance as hydrogen declines. In the absence of oxygen, the performance of this type of semiconductor hydrogen sensor is saturated and fails to recover to baseline values when sensing hydrogen in nitrogen gas (Figure 31). Tests indicate the need for the presence of oxygen for the sensor to perform accurately as it fails to return to baseline readings unless in the presence of air (Figure 18). Depending on where the device is located in the rumen, no oxygen may be present due to the reductive processes of the microbes within. The availability of alternative commercial hydrogen sensor needs to be explored as well as other possibilities for supplying oxygen to the sensor.

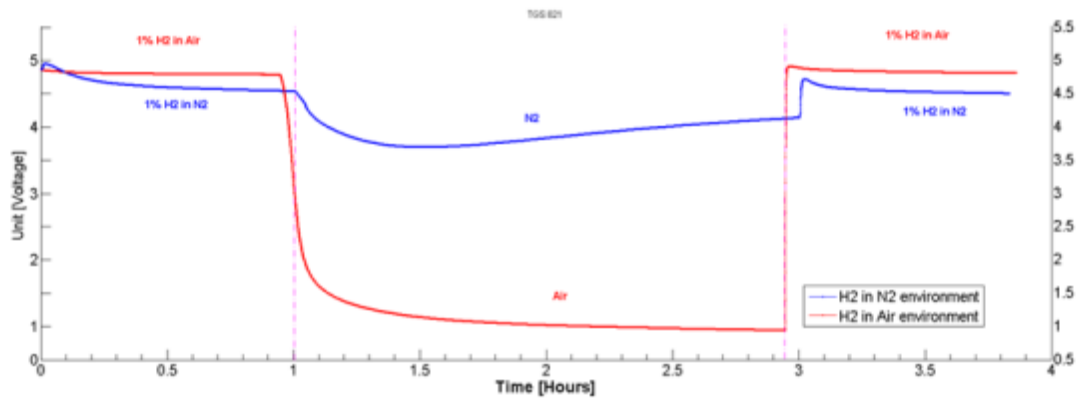


Figure 31. Studies under controlled conditions in the laboratory at RMIT testing the performance of the TGS821 hydrogen gas sensor with varying concentrations of hydrogen gas in a nitrogen or air atmosphere.

The new design incorporating finer and more dynamic membranes is resulting in more rapid responses to changes in target gas concentrations. The current prototype enables the use of 150µm membranes and possibly finer ones that possess much faster gas diffusion rates as compared to previous PDMS membranes purchased from a commercial manufacturer (> 300µm) which covered much of the surface of the barrel of the CRD. The integrity of the finer membrane is protected by the end-cap design with no failures experienced in the latest series of testings and experiments. Silicone adhesive binds the membrane to the rim of the gas sensor as well as to the end-cap assembly and thereby providing a barrier to rumen fluid gaining entry to the electronics within the CRD. On earlier tests a mesh barrier was incorporated between the gas sensor and the PDMS membrane to protect the unit from herbage material from piercing the membrane.

Utility of the device to discriminate difference between high and low methane animals

Cattle experiment with CH₄/CO₂ sensor:

Fistulated cattle at Lansdown Research Station were placed in respiration chambers whilst being treated with the methane inhibitor which was withdrawn on the final day. Expired methane gas concentration and IR methane gas concentration were recorded and compared (Figure 32). There tended to be an inverse relationship between expired methane production rate (trend line of methane concentration) and methane concentration in the rumen. When methane production was increasing after feeding, concentration of methane in the rumen was declining due to dilution by carbon dioxide gas being generated from increased fermentation. While this overall relationship appeared true and there was a positive correlation between average methane concentration in the rumen over a day and the amount of expired methane in individual animals, the r^2 correlation for the group was low (0.21, Table 1).

Table 1. Measurements of methane production by respiration chamber and methane concentration in the rumen by IR gas-sensing device.

Animal	(+ chloroform)		(-) chloroform	
	CH ₄ production (g/d)	Av. rumen CH ₄ (%)	CH ₄ production (g/d)	Av. rumen CH ₄ (%)
621	132.6	16.95	166.4	17.42
622	160.3	20.10	165.9	21.30
625	125.9	18.51	137.8	19.08

It is recognised that there may be a need to incorporate a reference gas in the rumen such as sulphur hexafluoride (SF₆) to optimise results from this type of technology. Sensors, capable of measuring SF₆ simultaneously with methane and carbon dioxide have recently become available commercially and to refine future developments of intra-ruminal devices may require the inclusion of one of these sensors and pressure measurements taken in experimental cattle at Lansdown.

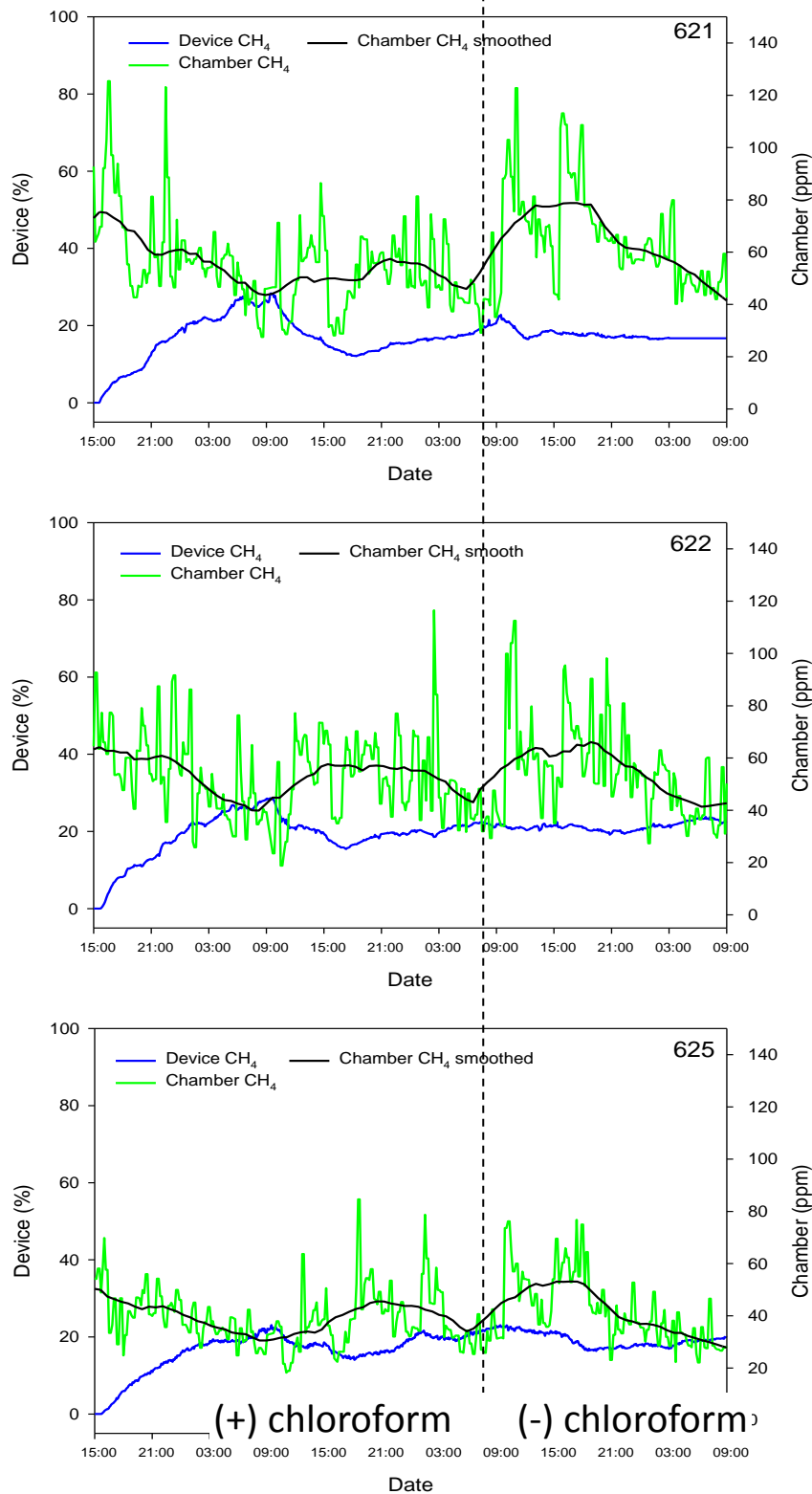


Figure 32. Methane concentration measured with the IR gas-sensing device and measured as eructated gas via the respiration chamber in cattle fed with and without chloroform to alter methane production on alternative days

Sheep experiment with CH₄/CO₂ sensor:

Similar to the experiment in cattle reported above, there tended to be an inverse relationship between expired methane production rate (trend line of methane concentration) and methane concentration in the rumen (Figure 33). When methane production was increasing after feeding, concentration of methane in the rumen was declining due to dilution by CO₂ gas being generated from increased fermentation. Conversely later in the day when fermentation rate and methane production were declining, there was an increase in methane concentration in the rumen relative to CO₂ concentration. This occurred when the sheep was fed either 1000g or 500g per day.

In the cattle trial, there was a positive correlation between average daily intra-ruminal methane concentration and methane production when methanogens is was inhibited with chloroform. In the sheep trial the opposite occurred when a reduction in methane production was induced by a decrease in feed intake. When the sheep was fed 1000g (day 1) the mean CH₄ concentration as measured by the IR gas sensing device for that period was 26.0% and on day 2 (500g pellets) the mean CH₄ concentration was 30.8%. Production of CH₄ as measured by the chambers was 23.7g on day 1 and 14.9g on day 2. This was probably due to the different rates of CO₂ production in the rumen relative to methane formation in the two different approaches (inhibition with chloroform or reduction by restricting intake) we used to reduce methane.

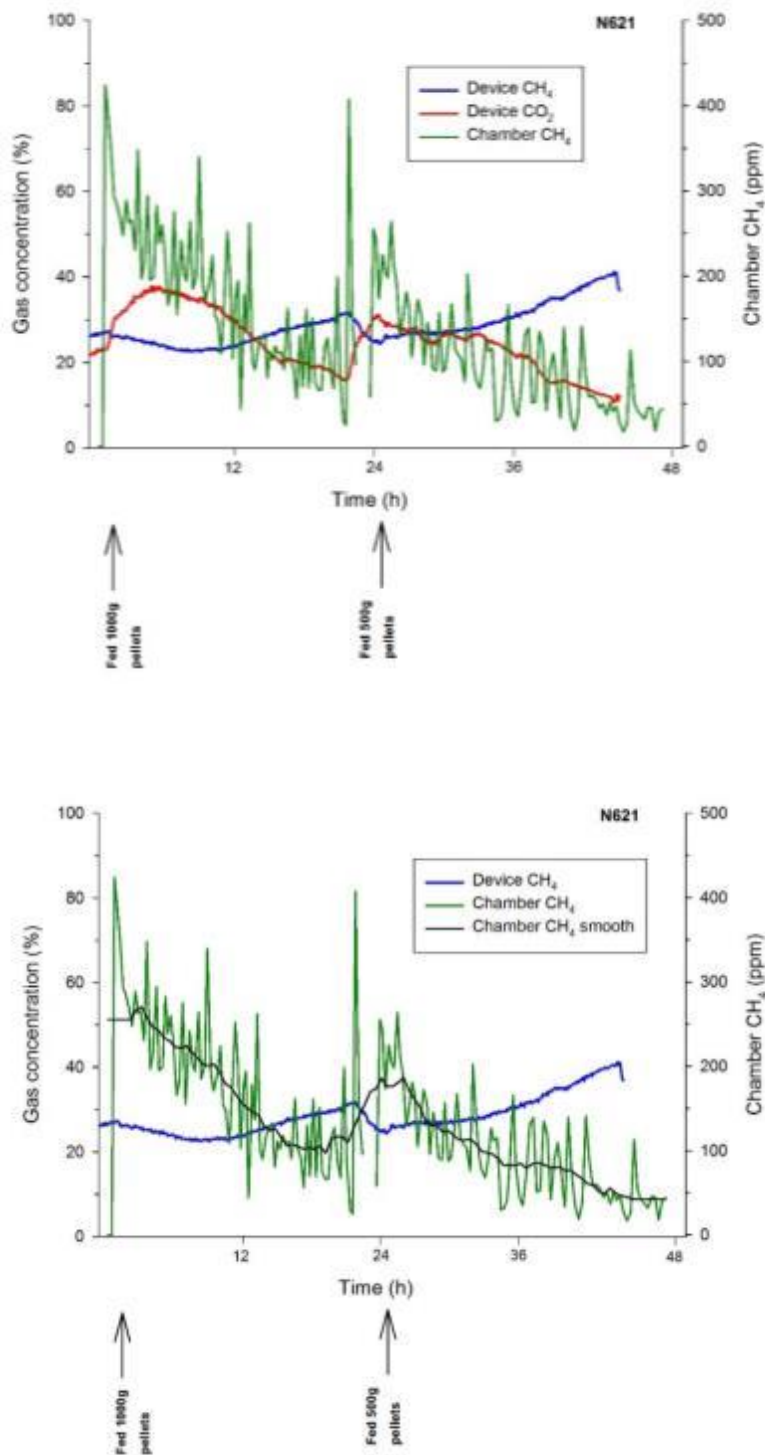


Figure 33. Methane concentration measured with the intra-ruminal device and measured as eructated gas via the respiration chamber in a sheep fed 1000g or 500g of Lucerne pellets on alternative days. Top panel also shows intra-ruminal CO₂ concentration. Bottom panel also shows the trend line for expired methane concentration.

Utility of the device to discriminate difference between high and low hydrogen emitters

Cattle experiment with Figaro H₂ sensor

Fistulated cattle at Lansdown Research Station were placed in respiration chambers whilst being treated with the methane inhibitor which was withdrawn on the final day. Expired hydrogen gas concentration and IR hydrogen gas concentration were recorded and compared (Figure 34). Large peaks of hydrogen (50-80 ppm) were recorded as eructated gas in the respiration chamber in association with feeding during methane inhibition with chloroform. These surges in hydrogen production were also recorded by the IR sensors (2500-14000 ppm) When chloroform was withdrawn, eructated H₂ gas measured by the respiration chamber was less than 20 ppm throughout the day. The IR H₂ sensors in two of the animals (502 and 510) also reflected little increase in H₂ concentration from the baseline) during the absence of chloroform although a large increase in hydrogen was measured in one animal (512) when no change was detected by the respiration chamber. The reason for the discrepancy is not known but may indicate spoilage of the sensor in the rumen or saturation due to lack of oxygen which is required to regenerate the sensor.

The testing of the redesigned TGS821 hydrogen sensor in the rumen of cattle undergoing respiration chamber measurements in Townsville has provided new insights into the levels of hydrogen (ranging from 1000-5000 ppm) within the rumen during the course of a day when methane is not inhibited (Figure 34) in cattle being fed hay and grain supplemented diets. These measurements of *in-rumen* hydrogen provide the first physiological insights into the release and utilisation of hydrogen in the rumen as the levels measured by respiration chambers are undetectable for the majority of the day due to dilution in the atmosphere of the chamber and insufficient sensitivity of gas sensors used in respiration chambers.

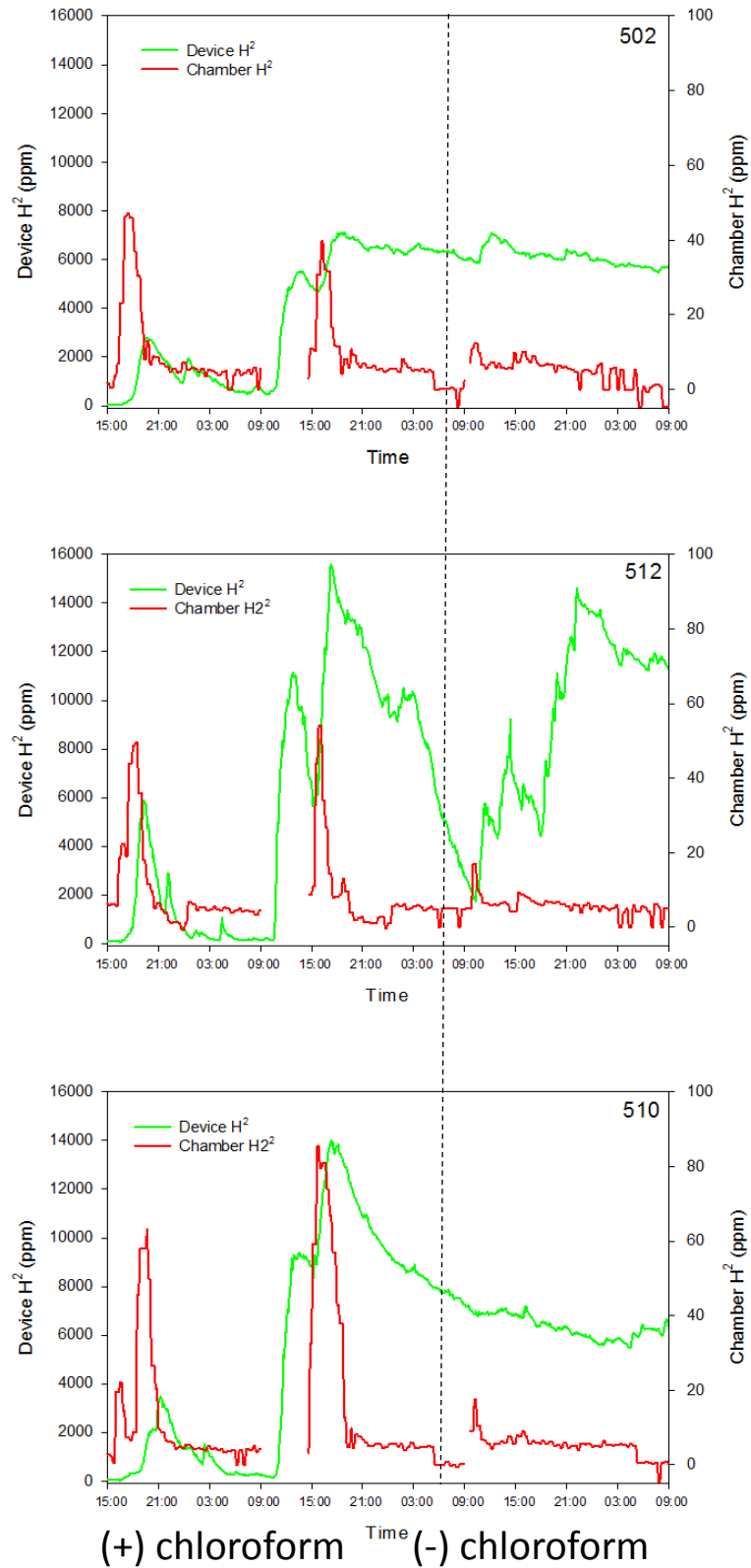


Figure 34. Hydrogen concentration measured with the intra-ruminal device and measured as eructated gas via the respiration chamber in cattle fed with and without chloroform to alter methane and hydrogen production on alternative days

Sheep experiment with Figaro H₂ sensor

Fistulated sheep at Chiswick Research Station were placed in respiration chambers and fed 1000g or 500 g Lucerne pellets on alternate days to determine whether differences in hydrogen production could be detected by the IR gas-sensing device. Expired hydrogen gas concentration and IR hydrogen gas concentration were recorded and compared (Figure 35). Large peaks of hydrogen (120 ppm) were recorded as eructated gas in the respiration chamber in association with feeding 1000g Lucerne in two (512 & 513) of the four animals. These surges in hydrogen production were also recorded by the IR sensors but the concentrations were lower than expected. The IR H₂ sensors in two of the animals (502 and 517) recorded increase in hydrogen which were not detected in the respiration chamber gases. The reason for the discrepancy is not known but may indicate periods of rumination and increase hydrogen production which are below the levels of detection by chamber measurements.

The IR H₂ sensing device studies in both cattle and sheep indicate that levels of H₂ in the rumen throughout the day are mostly not detected by chamber measurements as they are below the limits of detection due to dilution factors of the eructated gases in the chamber before they are measured by external sensors. This is a very important finding as it demonstrates that quantitative measurements of H₂ from open-circuit chamber studies underestimate H₂ production in the rumen. More accurate measures of H₂ production would be achieved by measuring accumulation of hydrogen in closed-circuit respiration chambers or portable accumulation chambers (PACs). A practical outcome of the project is that IR H₂ sensing device would be very suitable for measuring the concentration of accumulated H₂ of in PACs in selection for high and low methane emitting animals. Two different H₂ sensors (electrochemical SGX-e2v® sensor; Figaro TGS821 semiconductive sensor) and associated platforms have been trialled in animals and these studies demonstrate there are limitation to their long term use in the rumen.

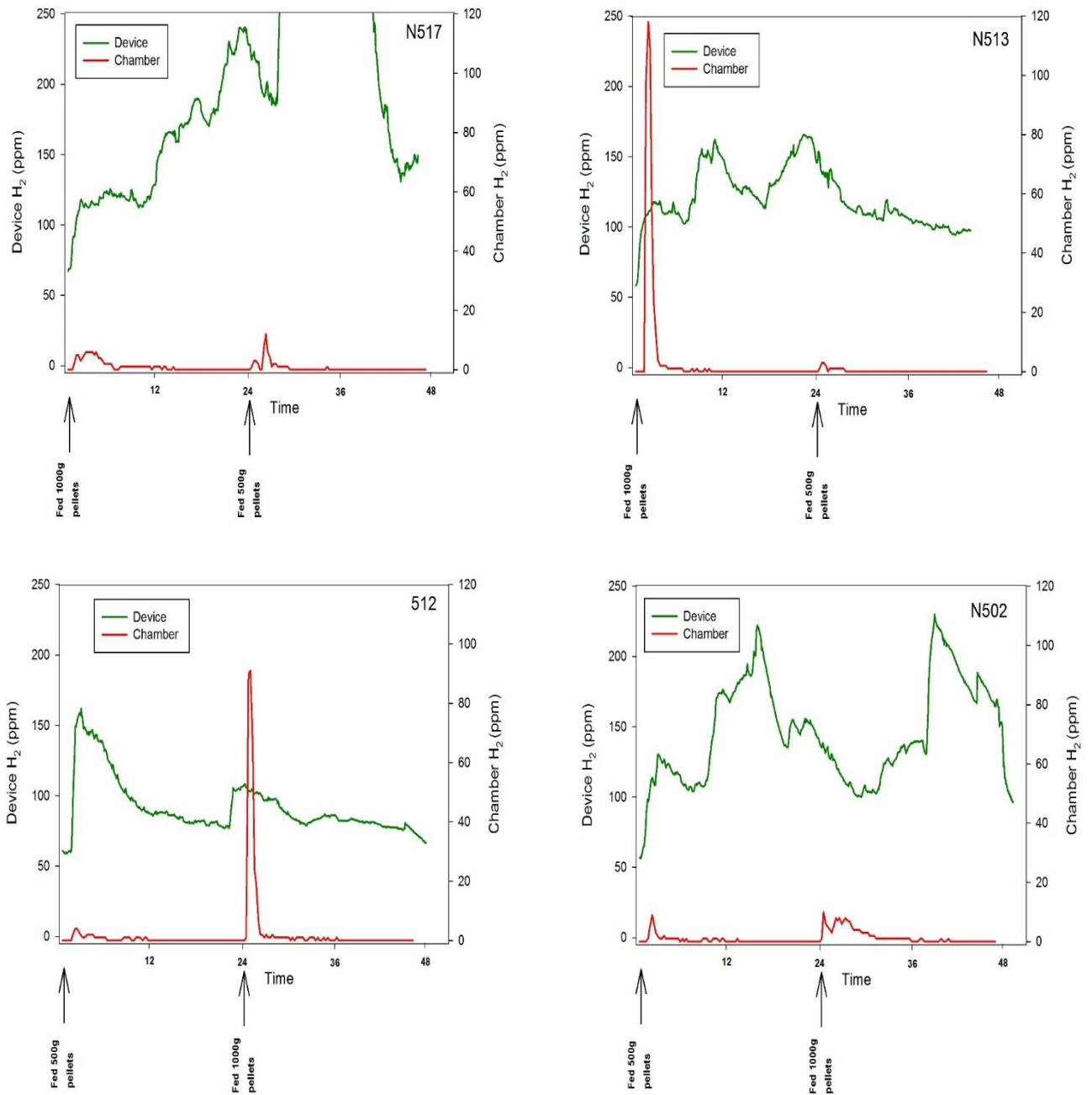


Figure 35. Hydrogen concentration measured with the intra-ruminal device and measured as eructated gas via the respiration chamber in sheep fed 1000g or 500g of Lucerne pellets on alternative days.

Improving the Radio Communication Features and Data Relay

The schematic below (Figure 36) shows the current configuration for data recording and transmission from the IR device of animals at a CSIRO Research Station to a remote personal computer at CSIRO Queensland Biosciences Precinct, Brisbane.

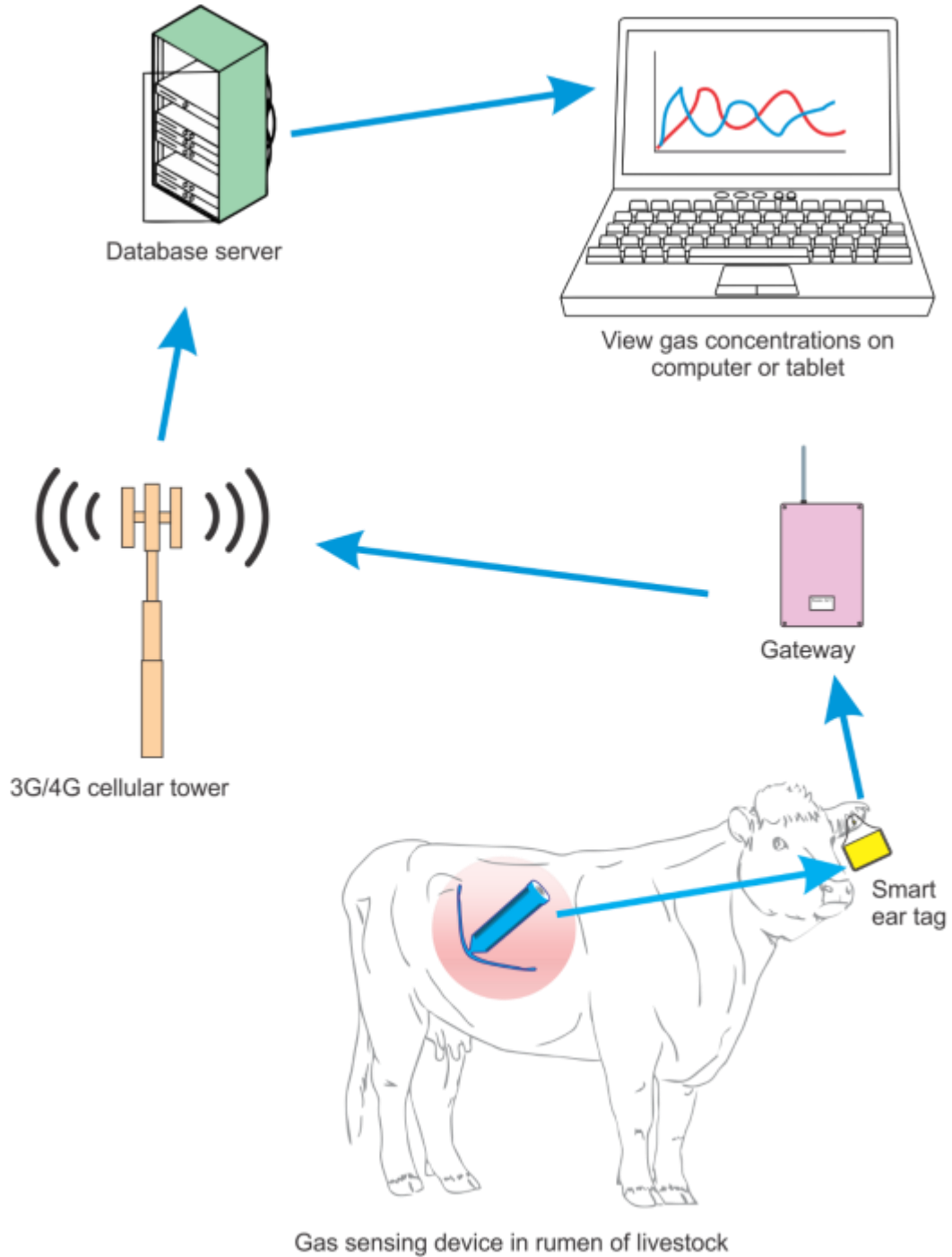


Figure 36. Overview of system architecture

Relay experiment 1: Smart ear tag on the steer's ear, IR device with the on-board chip antenna and CSIRO gateway

The IR device was placed into the rumen and the ear tag node attached to the steer's ear. The Receive Signal Strength Indicator (RSSI) values of periodic broadcasts from the relay ear tag were recorded by the IR device. The number of real-time data packets received by the gateway was also recorded. When the rumen device was inside the rumen it was immediately evident that the signal strength was poor since commands issued from the base no longer received responses. This is typical of poor round-trip (gateway – ear tag - rumen device – ear tag – gateway) link quality. Communications directly from the ear tag to the gateway were possible but still degraded. This was likely due to the combination of distance of the ear tag to the gateway and attenuation due to the proximity of the animal's body (ear, head mostly).

Relay Experiment 1 was conducted over a period of approximately 1.5 hours. During this period only 5 RSSI packets of data were received by the rumen node from the relay and only 4 data packets from the rumen node were successfully relayed to the gateway as seen in Figure 37. Due to the poor performance, additional configurations (Experiments 2-5) were then tested.

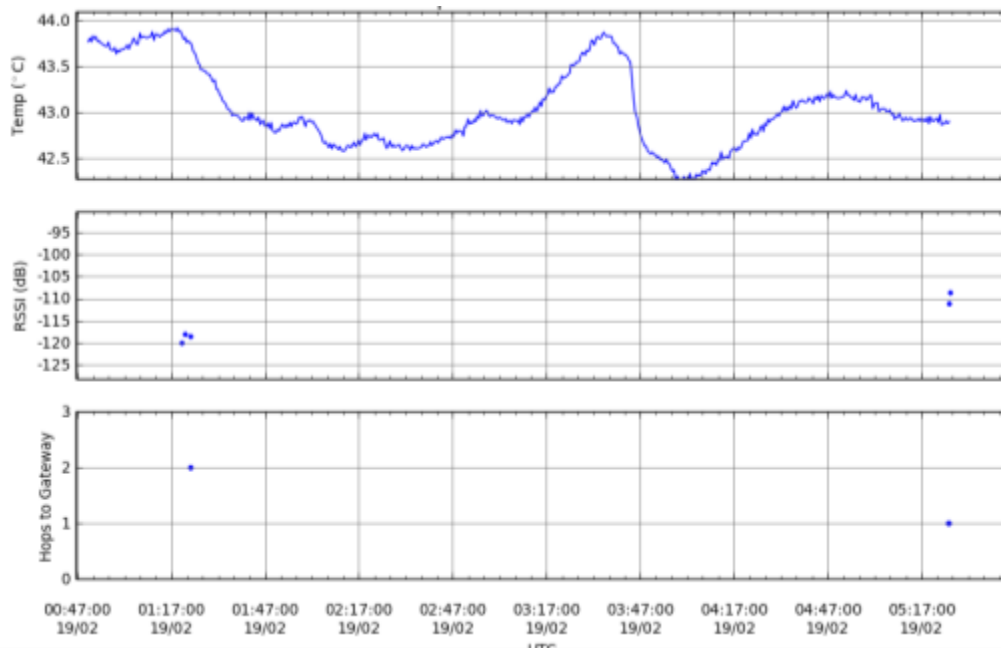


Figure 37. Temperature data as recorded in the rumen (top), the RSSI from packets between the relay node on the ear and the rumen node (middle), and the number of hops to the gateway (bottom)

Relay Experiment 2: CSIRO's smart ear tag on steer's fistula, intra-rumen device with the on-board chip antenna and CSIRO gateway

Relay experiment 2 ran for 17 hours 42 minutes. During this experiment the animal was closer to the gateway than during Relay Experiment 1 and the ear tag placed on the side of the animal. This allowed periods where the rumen device could directly communicate to the gateway (i.e. 1 hop to the gateway). This is clearly evident when the relay ear tag device ran out of power (during 16:23 to 20:19 in

Figure 38) and numerous packets arrived directly to the gateway (i.e. hop count = 1) but there was no RSSI data for the same period since the relay ear tag was not beaconing RSSI packets. For the periods where the ear tag was powered, the RSSI between the rumen device and the ear tag was mostly symmetric, though varied over time likely due to movement of the device within the rumen and the amount of matter (water, grass, etc) varying.

In conjunction with the real-time data broadcasts from the IR rumen device, all data is also recorded to onboard (flash) memory in a compact, partially compressed binary format. This memory is arranged in 256 byte “pages” which can be downloaded via 8 RPC (Remote Procedure Command) packets. This provides a method for retrieving any data that may not have been received in real-time. This is referred to as Delay Tolerant Networking (DTN) as it allows all data to be safely delivered to the base in a delay-tolerant manner. Prior to this experiment starting, 1084 pages of data had been stored, however only 408 had been downloaded. Therefore during this experiment the gateway attempted to retrieve the stored data, however the DTN requires a robust bi-directional communications channel which was not present with this configuration. As such, there were only brief periods where connectivity was sufficient to download pages, resulting in 215 pages being downloaded during the experiment. Over the same period however, the device only stored an additional 208 pages indicating that the DTN can in fact recover missed data, despite the poor connectivity experienced in this configuration.

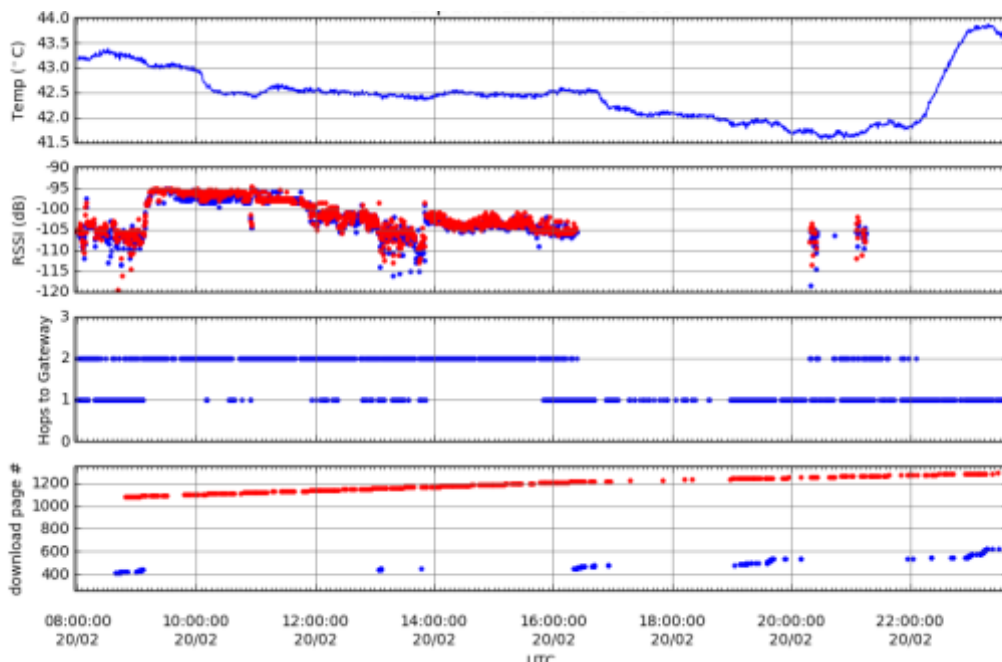


Figure 38. Rumen temperature recorded by the node on flash (top). Second top graph shows RSSI recorded by the rumen device from relay node packets (blue) and RSSI from rumen device packets recorded by the ear tag device (red). The hop count is shown on the second bottom and the bottom graph shows the current page written to flash (red) and the current page downloaded (blue).

Relay Experiment 3: CSIRO's smart ear tag on sheep's fistula, intra-rumen device with the on-board chip antenna and CSIRO gateway.

Relay experiment 3 was a multi-day experiment conducted on a fistulated sheep. The attenuation by the sheep's body was less than that of the steer, however, communications to the chip antenna from the ear tag was still too poor for reliable DTN. Despite this, many real-time data readings were successfully relayed to or directly received by the base.

Relay Experiment 4: CSIRO's smart ear tag on sheep's fistula, intra-rumen device with the ¼ wave whip antenna and CSIRO gateway

Relay experiment 4 ran for 18.5 hours and demonstrated reliable relaying of real-time data and the successful retrieval of all archived data via DTN due to the robust bi-direction communications. This is the ideal system performance and the goal for relay performance when the ear tag is on the ear of any livestock animal.

Relay Experiment 5: CSIRO's smart ear tag on sheep's ear, intra-rumen device with the ¼ wave whip antenna and CSIRO gateway

Relay experiment 5 ran from 20/3/2014 03:00 UTC to 22/3/2014 09:00 UTC during which a few configurations were briefly trialled. Initially the ear tag was attached to the fistula plug as per experiment 4 and shortly thereafter shifted to the ear (approximately 5:30 UTC). Figure 41 shows the dramatic reduction in RSSI due to the attenuation of the animal's body after the tag was moved to the ear. During the period up to 21/3/2014 00:20 UTC the receive performance was poor, however a reasonable portion of real-time data from the rumen device was received by the gateway anyway. The relay ear tag's antenna was then exposed outside the case at approximately 21/3/2014 00:20 UTC, after which the RSSI improved, permitting more robust delivery of real-time data but still not sufficient for DTN to retrieve all archived data.

During the 24 hour period from 21/03/2014 00:20 UTC to 22/03/2014 00:20 UTC, 70% of real-time data packets were successfully relayed to the gateway, demonstrating that relaying of rumen data via an ear tag on the ear is a viable strategy for enhancing the data delivery from then rumen device.



Figure 39. Configuration for Relay Experiment 5: Ear tag in the ear of a sheep with whip antennae extended and rumen node in the CRD with a whip antenna

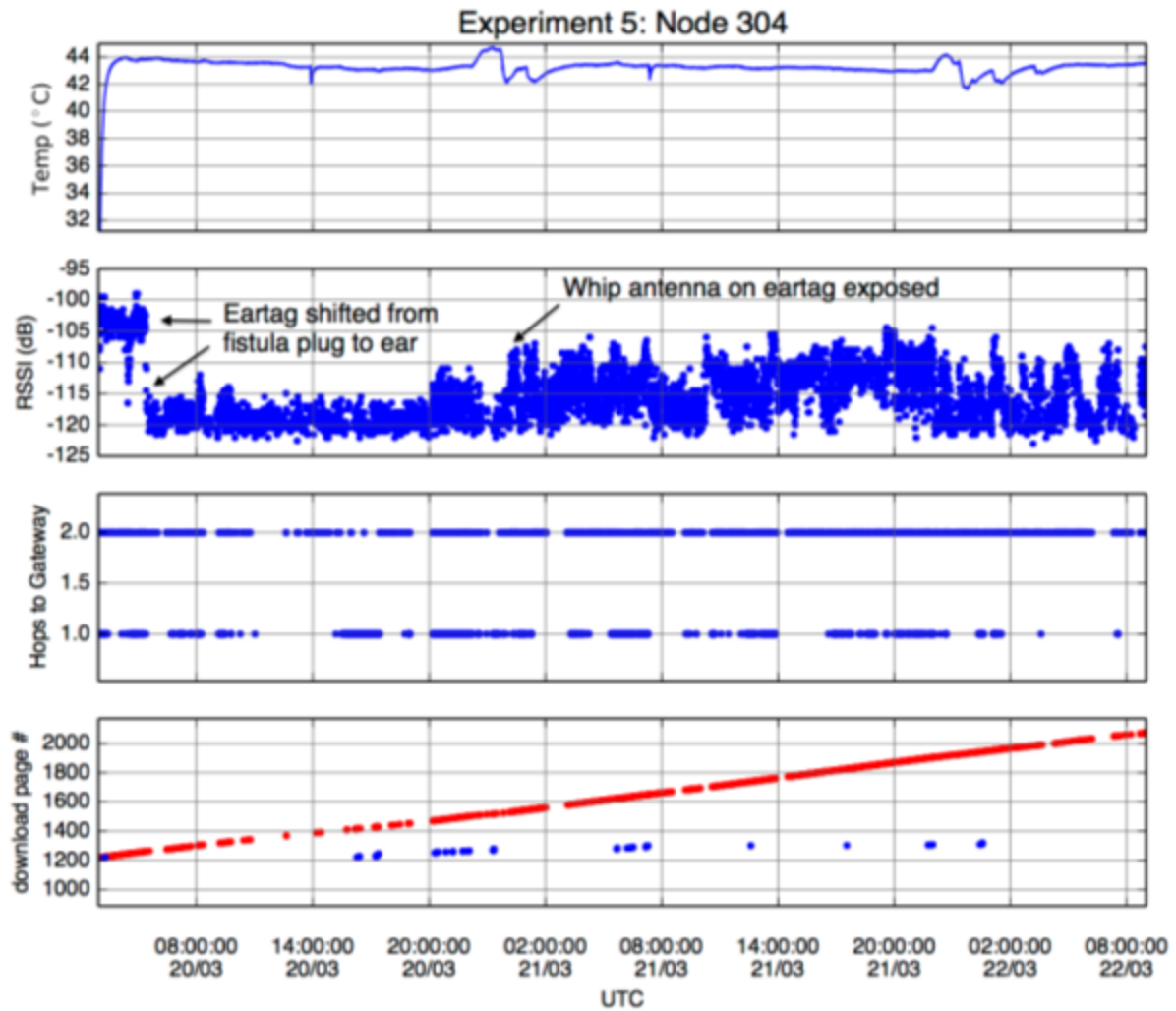


Figure 40. Experiment 5: Rumen temperature recorded by the node on flash (top). Second top graph shows RSSI recorded by the rumen device from the ear tag. The hop count is shown on the second bottom and the bottom graph shows the current page written to flash (red) and the current page downloaded (blue).

Managing the Energy Requirements of the IR Gas-sensing Device

Developing an Energy Management Supervisor Module

An energy saving sampling strategy has been devised based on the premise that changes in temperature tend to indicate activity in gas concentrations. This assumption is supported by a previous dataset in which sampled all sensors, periodically every 5 minutes over the course of 5.4 days (generating 1554 samples of each sensor). This is visible as the blue traces in figure 41 where fluctuations in the absolute difference of temperature (top) correspond with significant changes in the CO₂ and CH₄ concentrations.

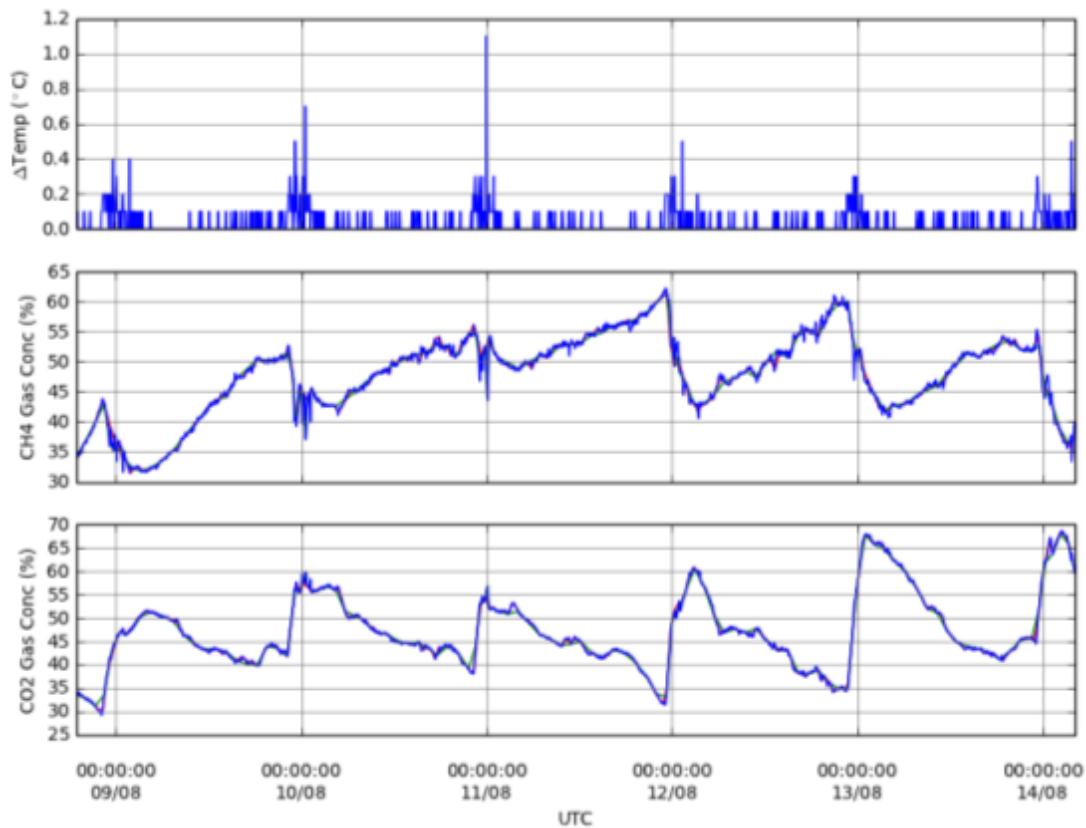


Figure 41. Absolute temperature difference between samples (top panel), CH₄ (blue, middle panel), and CO₂ (blue, bottom panel) gas concentrations as measured every 5 minutes. Periodic sub-sampling every 30 mins (red) and by the dynamic sampling strategy (green). Note, the red and green traces are difficult to discern indicating that both strategies represent the real data fairly well.

The dataset was also sub sampled such that gas concentrations were read every half hour (i.e. every 6th data point was used) and so required only 259 samples (red traces, figure 41 & 42). With the assumption that gas readings dominate the lifetime of the device, we estimate that this strategy would extend the lifetime of the device by approximately 6 times. The disadvantage of subsampling is the loss of high frequency transitions; this is evident in estimated gas concentrations in figure 42 with the red line which represents the periodic sampling strategy atop the blue points which are the actual 5 minute-interval samples. The “loss of information” is measured by the mean square error (MSE) across all actual recorded points to the interpolated points from the subsampling strategy. The periodic strategy demonstrated a MSE of 0.686 % for CH₄ and 0.199 % for CO₂ respectively and proved to be a very reasonable strategy for significantly reducing the power while faithfully reconstructing the gas concentrations for most of the experiment. Ideally however, a dynamic sampling strategy should capture high frequency transitions as well or better with less samples.

The dynamic strategy (green traces, figure 41 & 42) uses fluctuations of the temperature (Δ_{Temp}) to modify the sampling period from 5 minutes (P_{min} , which is fast as possible given the dataset), through to every 1.5 hours, P_{max} . However the strategy has an inbuilt tendency to fall back to the default period, $P_{default}$, of 30 minutes if temperature variation is neither too frequent nor too infrequent. The sample period, P_{sample} , is governed by 3 parameters:

- α The rate at which the sampling frequency increases. Range [0,1]
- β The rate at which the sampling frequency decreases. Range [0,1]
- γ The decay rate towards the default sample period (30 minutes). Range [0,1]

and can be expressed by the equation:

$$P_{sample} = P_{default} + [\beta 2P_{max}(1 - \Delta_{Temp}) - \alpha P_{max}]$$

Note that P_{sample} is clipped to reside within P_{min} and P_{max} . A parameter sweep between the range of [0,1] in 0.01 step intervals was performed for each of α, β, γ and the MSE and number of samples for each combination recorded. Figure 43 shows the results of all combinations of parameter values for CH₄ measurement. All dynamic strategy parameter combinations resulted in performance that was at least as Pareto efficient (gray coloured) to the simple 30-minute sampling strategy (green square). The trade-off between number of samples and error is easily visible as a Pareto front, where one can choose anywhere between the extremes of every sample for a minimal error, through to sampling only every 1.5 hours (87 points) but with more significant error (particularly in high transition regions). Compared to the fixed periodic strategy, there were numerous dynamic sampling strategies which were more efficient *and* more accurate than the fixed strategy (Solutions in Figure 42 shown in red). For example, a solution with $\alpha = 0.46$, $\beta = 0.26$, $\gamma = 0.91$, demonstrated a MSE of 0.617% for CH₄ using only 122 samples.

This indicates that a more accurate representation of the true methane concentration can be obtained with significantly less samples. In theory, this dynamic sampling strategy should enable the energy source to last more than twice (212%) as long as the fixed sampling strategy and furthermore, more faithfully represent the dynamic diurnal variation typical to that observed in this experiment.

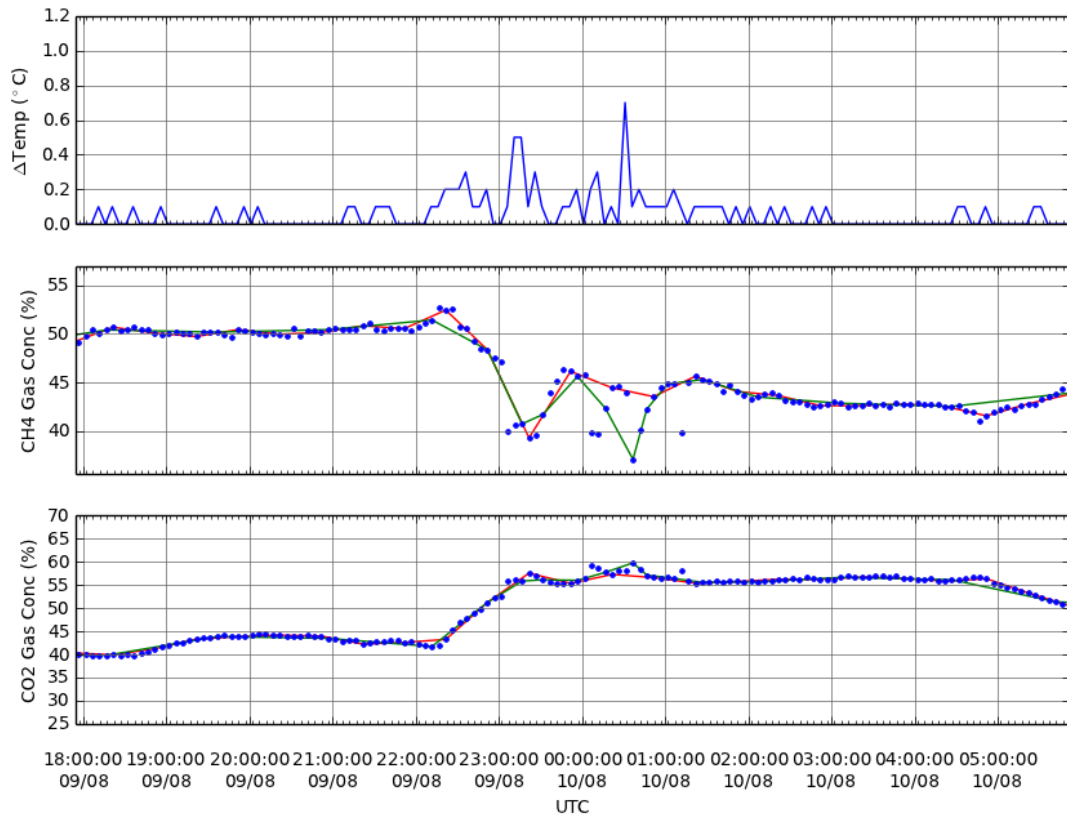


Figure 42. Zoomed in portion of figure 41, highlighting that the dynamic sampling strategy (green) provided a better representation of the higher frequency events than periodic sampling (red).

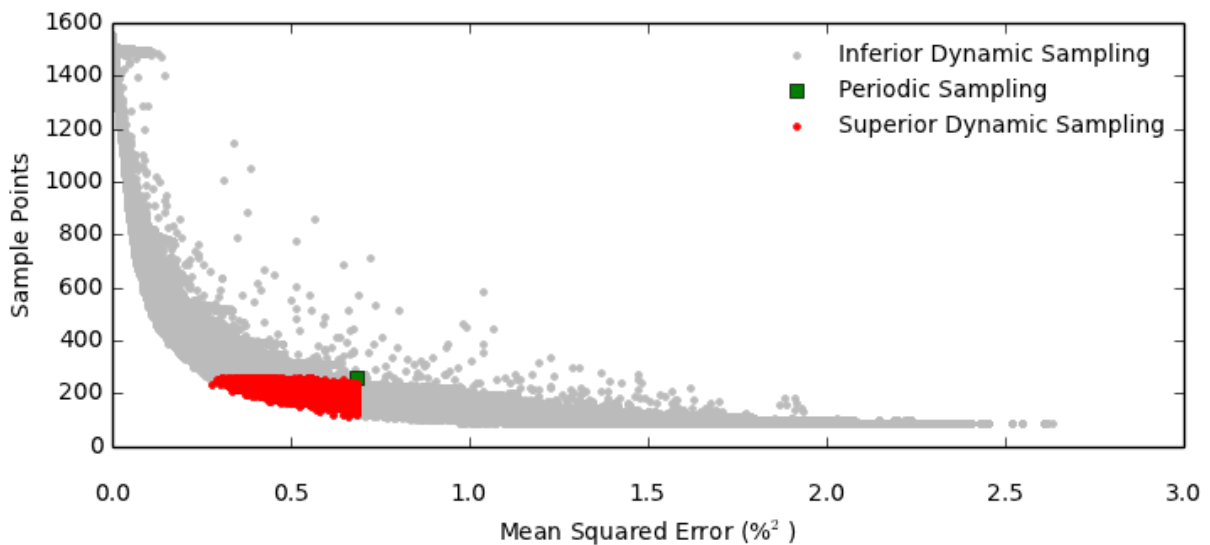
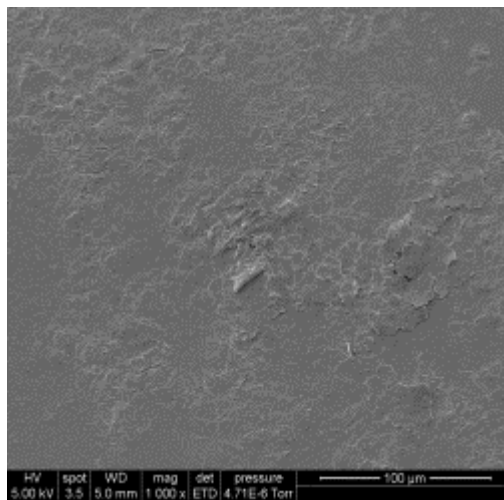


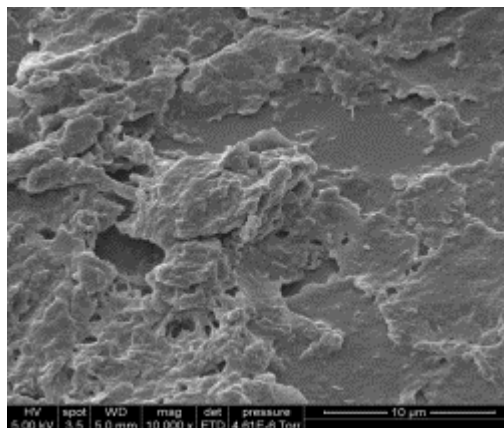
Figure 43. Results of the parameter sweep for the dynamic sampling strategy. MSE versus the number of sample points taken. The red dots represent solutions (dynamic strategy with various parameter configurations) which outperform (i.e. dominate) the periodic strategy.

Testing microbial colonisation of PDMS membranes in the rumen

As part of the collaboration with RMIT (project B.CCH.6220) PDMS membranes were suspended in the rumen for periods up to a month to test the rate and extent of microbial colonisation. Colonisation analysis of the membranes was undertaken by staff at RMIT. Electron microscopy was used to visualize colonization and DNA analysis undertaken to characterize the different microbial populations present. Details of the results are presented in the Final Report for project 01200.006; B.CCH.6220. Marked differences in microbial colonization were observed at 14 days (Figure 44) between the control (no silver nanoparticles) and the 0.25%Ag-PDMS membranes but significant colonisation had occurred at 1 month in the Ag impregnated membranes.



Day 14 (0.25%Ag-PDMS)



Day 14 (Control)

Figure 44. Electronmicrographs of silver impregnated PDMS membranes placed in the rumen compared with controls (no silver).

4. Conclusions

The livestock industries required a technology to rapidly and accurately measure enteric gas emissions from large numbers of individual animals. At the commencement of the project, no such technology existed and there are limitations regarding the application of technologies presently available. A new technology/device would enable researchers and producers to validate methane mitigation strategies in grazing ruminants. Intra-rumen devices incorporating gas sensors and a wireless sensor network platform have been developed in the project that log concentration of methane, carbon dioxide and hydrogen gas in the rumen for research purposes. The devices are equipped with a novel gas permeable membrane embedded with silver nanoparticles which allows the diffusion of the target gases while blocking corrosive hydrogen sulphide. Real time data from the capsule in the rumen can be relayed via an ear tag to a remote personal computer using the public G3 network communication system. The longevity and accuracy of the device is compromised by the corrosive environment in the rumen. The project demonstrated that measurement of hydrogen concentration in the rumen appears to reflect production rate which currently cannot be monitored by conventional methods such as respiration chambers. It is possible that average hydrogen concentration in the rumen may correlate with a low and high methane emissions phenotype as an underpinning mechanism. Recent studies in New Zealand indicate that production and availability of hydrogen in the rumen may determine whether an animal is genetically a low or high methane emitter. Therefore the current hydrogen sensor could be deployed in portable gas accumulation chambers to obtain more accurate measurements of hydrogen production in large groups of sheep. A relationship between methane concentration and methane production could not be established. Measurement of a marker gas released at a constant rate in the rumen will be needed to estimate methane production for assessment of methane abatement methodologies and genetic selection programs for methane. Measurement of methane yield and concentration should allow emissions intensity, total emissions and efficiency of rumen fermentation processes to be predicted.

The gas-sensing devices have provided the first continuous record of physiological data relating fermentation gases in the rumen and effects of diet and feeding events. This has provided a fundamental basis for understanding the mechanisms which might contribute to a low and high methane phenotype. In addition the monitoring of fermentation gases provides an index of rate and extent of fermentation which may assist in identifying animals that have more efficient and productive rumens. The measurement of temperature and pressure in the rumen by the device could also be used in the future to identify eating, ruminating and grazing behaviour in the animal which may also contribute to differences in productivity particularly in the more extensive and harsh grazing systems of northern Australia. The gas sensing device could also be deployed for measuring expired gases at a much cheaper cost than current technologies on the market. Therefore the Australian ruminant livestock industries could benefit from the development of this tool in the future for research on enhancing productivity.

5. References

- Johnson, K, M. Huyler, H Westberg, B Lamb, & P. Zimmerman.1994a. Measurement of methane emissions from ruminant livestock using aSF6 tracer technique. *Env. Sci. Technol.* **28**:359–362.
- Johnson, KA, M.T. Huyler, H.H. Westberg, B.K. Lamb, & P. Zimmerman.1994b. Measurement of methane emissions from ruminant livestock using a sulfur hexafluoride tracer technique. In 'Energy metabolism of farmanimals'. EAAP Publication No. 76. (Ed. JF Aguilera) pp. 335–338. (Servicio de Publicaciones, Consejo Superior de Investigaciones Cientificas: Granada, Spain)
- Pinares-Patino, C.S., & H. Clark. 2008. Reliability of the sulfur hexafluoride tracer technique for methane emission measurement from individual animals: an overview. *Aust. J. Exp. Agric.* **48**:223–229.
- Pinares-Patino, C.S., C.W. Holmes, K.R. Lassey, & M.J. Ulyatt. 2007. Measurement of methane emission from sheep by the sulphur hexafluoride tracer technique and by the calorimetric chamber: failure and success. *Animal* **2**:141-148.
- Tremblay P, Savard M, Vermette J and Paquin R. 2006. Gas permeability, diffusivity and solubility of nitrogen, helium, methane, carbon dioxide and formaldehyde in dense polymeric membranes using a new on-line permeation apparatus. *J Membr.Sci.* **282**: 245-256.

6. Future research needs

The intra-ruminal devices can measure methane, carbon dioxide and hydrogen concentrations in the rumen accurately. This means the devices could be used in research animals to intensively study fermentation gas events in relation to techniques that reduce methane production or study the basic mechanisms that underpin high and low methane phenotypes. Measurement of a marker gas released at a constant rate in the rumen would be needed to estimate methane production for assessment of methane abatement methodologies and genetic selection programs. While the devices can log and transmit data for several weeks in the rumen the accuracy of the sensors declines over this period due to the harsh rumen environment. Therefore future research needs to focus on (1) building a new generation sensor that can withstand or matches the rigorous conditions of the rumen environment, or (2) other ways of protecting the current commercial sensors with gas scrubbers that clean the rumen gases before making contact with the sensor. The current device can be used as a cheap method for measuring expired gases that collect in portable accumulation chambers (PAC) or conventional respiration chambers where flow rate can be measured. The current device has provided a patent platform for the development of an ingestible human gas sensor device and is attracting global interest as the residence time in the gut (24-48 hours) means the current sensors remain stable. The human application appears attractive for further research and development.

7. Publications

- Bishop-Hurley, G.J., Paull, D., Overs, L., Valencia, P., Kalantar-Zadeh, K., Berean, K., Nour, M. and McSweeney, C.S. (2014). A Real-time Green House Gas Rumen Monitoring System for Free-ranging Livestock Presented at the "Joint ISNH/ISRP International Conference 2014 : Harnessing the Ecology and Physiology of Herbivores 8 -12 September 2014 Canberra Australia.
- Yao, C.K., Rotbart, A., Muir, J.G., Gibson, P.R., and Kalantar-zadeh,K. (2015). Human intestinal gas measurement systems: in vitro fermentation and gas capsules. Trends in Biotechnology (in press).
- Nour, M., Berean, K., Chrimes, A., Zoolfakar, A.S., Latham, K., McSweeney, C.S., Field, M.R., Sriram, S., and Kalantar-zadeh, K., Ou, J-Z (2014). Silver nanoparticle/PDMS nanocomposite catalytic membranes for H₂S gas removal. Journal of Membrane Science.
DOI:<http://dx.doi.org/10.1016/j.memsci.2014.07.047>
- Berean, K., Ou, J.Z., Nour, M., Latham, K., McSweeney, C.S., Halim, A., Kentish, S. and Kalantar-zadeh, K. (2014). The effect of crosslinking temperature on the permeability of PDMS membranes: evidence of extraordinary CO₂ and CH₄ gas permeation. Separation and Purification Technology 122, 96-104.
- Nour, M., Berean, K., Balendhran, S., Zhen Ou, J., Du Plessis, J., McSweeney, C.S., Bhaskaran, M., Sriram, S., Kalantar-zadeha, K. (2013). CNT/PDMS nanocomposite membranes for separating H₂ and CH₄. International Journal of Hydrogen Energy 38, 10494-10501.